AL.2.1986-54

A Preliminary Study Of The Chemical Composition And Combustion Efficiency Of A Sour Gas Flare

RMD Report 85/30

Alberta
ENVIRONMENT
Environmental Protection Services
Research Management Division

DDN 6010481

The logo represents the interdisciplinary and holistic nature of the Division's environmental research programs. Each of the five sections of the symbol represent comprehensive programs on air, water, land, humans, and their constant interaction. The sections converge to form a cohesive chain, characteristic of an effective research organization. This cohesive bonding makes the sections blossom into the environment in the form of a flower — an Albertan wild rose.

CANADIANA

DEC 1 8 1985

A PRELIMINARY STUDY OF
THE CHEMICAL COMPOSITION AND COMBUSTION EFFICIENCY
OF A SOUR GAS FLARE

RESEARCH MANAGEMENT DIVISION
Alberta Environment

Digitized by the Internet Archive
in 2016

https://archive.org/details/preliminarystudy00leah

For further information on reports published by the Research Management Division, contact:

Research Management Division
Publications Office
14th Floor, Standard Life Centre
10405 Jasper Avenue
Edmonton, Alberta
T5J 3N4

(403) 427-3946

This report may be cited as:

Leahey, D.M., H.G. Paskall, M.B. Schroeder, and M.J. Zelensky. 1985. A preliminary study of the chemical composition and combustion efficiency of a sour gas flare. Prep. for Alberta Environment, Research Management Division by Western Research, Division of Bow Valley Resource Services Ltd. RMD Report 85/30. 93 pp.

For further information on reports published by the Research Management Division, contact:

Research Management Division
Publications Office
14th Floor, Standard Life Centre
10405 Jasper Avenue
Edmonton, Alberta
T5J 3N4

(403) 427-3946

This report may be cited as:

Leahey, D.M., H.G. Paskall, M.B. Schroeder, and M.J.E. Zelensky. 1985. A preliminary study of the chemical composition and combustion efficiency of a sour gas flare. Prep. for Alberta Environment, Research Management Division by Western Research, Division of Bow Valley Resource Services Ltd. RMD Report 85/39. 93 pp.

A PRELIMINARY STUDY OF
THE CHEMICAL COMPOSITION AND COMBUSTION EFFICIENCY
OF A SOUR GAS FLARE

by

D.M. LEAHEY
H.G. PASKALL
M.B. SCHROEDER
M.J. ZELENSKY

Western Research
Division of Bow Valley Resource Services Ltd.

for

RESEARCH MANAGEMENT DIVISION
Alberta Environment

RMD Report 85/30

1985

This report is made available as a public service. The Alberta Department of Environment neither approves nor disagrees with the conclusions expressed herein, which are the responsibility of the author(s).

TABLE OF CONTENTS

Page

LIST OF TABLES vi

LIST OF FIGURES vii

ABSTRACT ix

ACKNOWLEDGEMENT x

1. INTRODUCTION 1
1.1 Literature Review 2

2. FIELD STUDY 11
2.1 Materials and Methods 11
2.1.1 Flare Feed Stream Compositions 11
2.1.1.1 Sampling Complications 15
2.1.2 Plume Sampling 17
2.1.2.1 Sampling Complications 20
2.1.3 Interviews of Sour Gas Plant Operators 20
2.1.4 Model Development 21

3. RESULTS AND DISCUSSION 22
3.1 Flare Feed Stream Evaluations 22
3.2 Plume Evaluations 27
3.3 Interviews of Sour Gas Plant Operators 33
3.3.1 Measurements of Volume Flow 33
3.3.2 Measurements of Composition 37
3.3.3 Flare Monitoring 38
3.4 Model Development and Testing 38
3.4.1 Theory 38
3.4.2 Model Evaluation 45
3.4.2.1 Wind Tunnel Tests 45
3.4.2.2 Acheson Data 51
3.5 Flare Efficiencies Through Model Use 57

4. CONCLUSION 64
4.1 Flare Efficiencies 64
4.2 Mercaptans and Heavy Metals 64
4.3 Interviews of Sour Gas Plant Operators 65

5. RECOMMENDATIONS 66

6. REFERENCES CITED 67

7. APPENDICES 70
7.1 Information Relating to Raw Data and Calibration 70
7.2 Questionnaire: Alberta Environment Flare Stack Emission Study 81
7.3 Derivation of Equations for Plume Rise, Plume Length and Plume Area 86

LIST OF TABLES

Page

1. Summary of Current Flare Test Programs 5

2. Flare Stack Parameters for Indicated Test Times 23

3. Compositions of Acid and Fuel Gases for the Indicated Periods (Mole Percent on Dry Basis) 24

4. Flare Gas Analysis (Mole Percent on Dry Basis) for Indicated Test Period 25

5. Concentrations of Indicated Species in Acid and Fuel Gas (ppm by Volume) 26

6. Trace Element Determination 28

7. Plume Analysis (Mole Percent on Dry Basis) for Indicated Test Period 29

8. Values of the Local Combustion Efficiency (E) and C/S Ratios Observed at the Indicated Distance from the Stack 32

9. Plume Analysis (ppm by Volume) 34

10. Range of Conditions Considered by Kalghatgi (1983) .. 46

11. Values of Molecular Weight, Stoichiometric Mixing Ratio, and Heating Contents for the Indicated Gases 47

12. Comparison Between Predicted and Observed Values of h_f/D_o for Indicated Gases 49

13. Comparison Between Predicted and Observed Values of α_B (Degrees) for Indicated Gases 52

14. Observed and Predicted Values of h_f/D_o, α_B and A/D_o^2 Together with Associated Values of R, β_o and n (Present Theory) 54

15. Observed and Predicted Values of h_f/D_o and α_B, using Kalghatgi's Theory (1983) 60

16. Comparison Between Efficiencies E as Observed at Downwind Distances of 2 m and Selected Parameters ... 62

LIST OF FIGURES

Page

1. Sketch of the Flame, Showing Plume Parameters Indicated by Kalghatgi (1983) 8
2. System for Determining Trace Species (Heavy Metals) . 14
3. System for Determining Trace Reactive Gas Streams (High Volume Sampler Method) 18
4. Variation with R of the Ratio of Flame Area to the Square of the Stack Diameter (Equation 12) 43
5. Variation with β_o of the Ratio of Flame Area to the Square of the Stack Diameter (Equation 11) 44
6. Comparison Between Predicted and Observed Values of h_f/D_o (Wind Tunnel Tests) 50
7. Comparison Between Predicted and Observed Values of α_B (Wind Tunnel Data) 53
8. Comparison Between Predicted and Observed Values of h_f/D_o (Field Tests) 55
9. Comparison Between Predicted and Observed Values of α_B 56
10. Comparison Between Theoretical and Observed Flames... 58
11. Comparison Between Predicted and Observed Values of A/D_o^2 (Adjusted for Downwash Effects) 59

ABSTRACT

The main purpose of this study was to evaluate flaring as a means of waste gas combustion. Secondary purposes included finding flare gas composition of trace metals and mercaptans as well as evaluating attitudes toward flaring activity. Interviews with sour gas plant operators provided information to evaluate attitudes.

A field program was conducted at a sour gas plant located near Acheson Alberta. Combustion efficiency, observed during four tests, at distances downwind of the flame were 100.0, 95.8, 89.1 and 22.3 percent, respectively. Complete combustion was thus achieved on only one occasion.

A theory is proposed which shows that flame geometry is a function of stack exit and meteorological parameters. Data relating to flame behaviour obtained from the Acheson field program as well as data in the literature confirmed the theory.

Because flare combustion efficiency is related to flame geometry, it was concluded that it too must be a function of stack exit and meteorological parameters. As these parameters are variable, combustion efficiencies must also be variable.

Three and two samples of acid and fuel gas, respectively, were analyzed for mercaptans and heavy metals. Mercaptans were also measured in the flare plume. Total measured mercaptans in the acid gas and flare plume were less than 315 and 31 ppm, respectively. Only two metals (P, Zn) had measured concentrations above 100 $\mu g \cdot m^{-3}$. These relatively high P and Zn values occurred in only one acid and one fuel gas sample, respectively.

Interviews with operators of sour gas plants demonstrated a general unawareness of potential difficulties that might be associated with flaring activities. These relate to loss of flame and low flare gas heat contents.

ACKNOWLEDGEMENT

This project was funded by the Research Management Division of Alberta Environment. Comments of Ms. Bonnie Magill of the Research Management Division and those of peer reviewers were very helpful.

1. INTRODUCTION

Flares are routinely used in the chemical and petroleum industry for the disposal of large quantities of unwanted flammable gases and vapours. They usually consist of jets of combustible gases emitted from a stack. The gases ignite and burn while diffusing into the atmosphere. There is evidence that flares are often not an efficient means of achieving combustion. This evidence takes the form of black smoke representing unburned hydrocarbons or detectable odours representing unburned noxious compounds such as hydrogen sulphide.

Two flare operating modes predominate in industry: an intermittent emergency release and a continuous low flow rate release. Flares associated with many chemical industries must be designed to cope with the maximum anticipated gas release caused by process upset or emergency shutdown. These situations seldom occur. While designed for high throughput the flare will be more commonly used for lower level continuous or semi-continuous releases caused by leaks in equipment, necessary venting of process, fugitive, storage and secondary emission sources. Volume throughput during an emergency release can be three orders of magnitude greater than those experienced on a routine basis. Therefore, flares must often be very flexible devices capable of high throughput and sustained operation at a high turn down ratio.

About 15 x 10^6 tonnes/year of waste gases are routinely flared in the U.S. (Joseph et al. 1983). Most of this is comprised of hydrocarbons. In Alberta, flares are employed for H_2S combustion. About 8.4 x 10^3 tonnes/year of sulphur are disposed on a continuous basis (Alberta Environment 1982). Estimates as to emergency releases in Alberta and elsewhere are not usually available as they are largely uncontrolled and infrequently monitored. Incineration or vapour recovery units can be used as an alternative to flaring for low flare rate releases. They tend however, to be less economical. No reasonable alternative exists for the combustion of massive emergency releases.

It is apparent that flares which are used to combust large quantities of waste material may have an appreciable adverse effect on the environment, if they are inefficient. Effectiveness of flaring, particularly for the lower continuous release rates, must be of major concern. Not only is the concern being expressed by the U.S. Environmental Protection Agency (EPA) but also by other national organizations such as the German Federal Minister of the Interior (FMI), the British Alkaline Inspector, and local organizations such as Alberta Environment and the California Air Resources Board. Various projects are underway. The German FMI recently sponsored an extensive test program and the EPA is sponsoring a series of studies, both separately and in conjunction with the Chemical Manufacturer's Association (Engineering Science 1983). Various industrial institutions, such as Shell Research Ltd., are also evaluating flaring operations specific to their applications.

This report presents a review of the literature regarding the study of flares. It also presents and discusses results of a field study into flare combustion efficiency at a sour gas plant, measurements of heavy metals in the flare feed stream, and summaries of brief interviews with sour gas plant operators. A simple methodology based upon energy conservation principles will be proposed in this report for purposes of assessing flare efficiency. A model needed to exploit this methodology will then be proposed and partially evaluated using data collected at Acheson and elsewhere. A more complete evaluation will not be undertaken because it is beyond the scope of this study.

1.1 LITERATURE REVIEW

Flaring efficiency as a measure of the degree to which combustion goes to completion can be evaluated in a number of ways. Most measures concern global and local combustion. It is of interest to discuss these concepts in the context of hydrogen sulphide.

Global efficiency for H_2S, for example, is defined following the manner of Siegel (1980) as:

$$U = \frac{M_i\ (H_2S) - M_o\ (H_2S)}{M_i\ (H_2S)} \times 100;$$

where: U = global efficiency (%)

$M_i\ (H_2S)$, $M_o\ (H_2S)$ = mass flow of H_2S in flare and off gases (i.e., plume) respectively.

Global efficiency is difficult to assess because it requires accurate measurements of plume velocity in order to assess mass flow. An alternate measure suggested by Siegel (1980) is the local efficiency E(%) as measured in the flare plume. The efficiency of conversion of reduced sulphur species to sulphur dioxide for example is defined by the equation:

$$E = \frac{\text{Amount of } SO_2 \text{ in flared gases} \times 100}{\text{Total sulphur in the flared gases}};$$

$$E = \frac{[SO_2]\ 100}{[SO_2] + [H_2S] + [COS] + 2[CS_2]}; \qquad (1)$$

where the square brackets denote mole percent. Concentrations of other compounds; except those shown, are assumed negligible.

Since an evaluation of local efficiency requires that only products in the off gases be measured, mass flow measurements are not needed, simplifying sampling requirements. It is fortunate that local efficiency measurements should be sufficient in most cases for evaluating combustion. This conclusion is supported by results of experiments conducted by Siegel (1980) using an array of 40 to 60 sample points for testing a 4.5 m high pilot flare with a 20 cm diameter. Joseph et al. (1983) also found from pilot studies that a single probe measurement should be sufficient to measure flare efficiency and detailed probe measurements may, therefore, not be necessary.

Very few studies have been conducted into actual performance of industrial flares. This is because of the many measurement problems encountered during attempts to characterize flare emissions. These include: (1) the effects of high temperatures and radiant heat on test equipment; (2) the meandering and irregular nature of flare flames due to winds and turbulence; and (3) the lack of suitable sampling locations due to flare heights. Because of these problems most studies have been done on small pilot flares.

Dubnowski and Davis (1983) have presented a review of major programs on flare combustion. Most of the discussed results are unpublished. They are summarized in Table 1. Each test program is classified as to the flare type tested, fuel type, range of operating conditions investigated, and sampling techniques used. Normal operating conditions referred to in the table means that adequate flare control is exerted for smoke suppression. This is usually done with the aid of steam injection systems to provide enhanced combustion. The following comments are pertinent.

Palmer (1972) Ethylene with its high propensity to smoke was used as the flare gas. Results of this test showed local combustion efficiencies in excess of 99.9 percent even when the flare was smoking.

Straitz (1978) Test results were not conclusive because of the limited sensitivity of the instrumentation. Estimates of combustion efficiency indicated poor combustion during smoking conditions.

Siegel (1980) This study was a very detailed evaluation of a pilot flare. Effects of variable steam rates, flare gas densities and wind velocities were assessed. But only large heat content (55 $MJ \cdot m^{-3}$) gases comprised mostly of hydrogen were investigated.

Lee and Whipple (1981) There were difficulties with the continuous sampling techniques. Results from integrated (grab) sampling demonstrated combustion efficiencies greater than 99 percent. Uncombusted carbon was observed in gas pockets (eddies)

Table 1. Summary of Current Flare Test Programs

Flare Test Program (Ref.)	Flare Type	Flare Gas Composition	Heating Value ($MJ \cdot m^{-3}$)	Steam Control (kg/kg)	Flow Rate	Tracer	Continuous Sampling/ Analysis	Integrated (grab) Sampling	Efficiency Range Normal Op. Cond.	Comments
Palmer (1972)	1.3 cm dia. Stream-Assisted Model Flare	Ethylene	54	0-.3	15 45 75 $m \cdot s^{-1}$	helium	none	yes	When detectable less than .096% ethylene uncombusted	Objective was to investigate use of a tracer for possible evaluation of full-size flares
Straitz (1978)	Pilot Stream Flares 5.0, 7.6, 15.2 cm	Natural Gas & Propane		0 to quenching		none	yes single probe (cooled)	none	>99% 75% during smoking	Range sensitivity of instrumentation limits validity of results
Siegel (1980)	Flargas ES-6 Conicol design 20 cm dia. steam-assist Pilot Flare	High hydrogen concut refinery gases (.5-1.8 $kg \cdot m^{-3}$)	~55	0-1.73	max 3.3 $t \cdot h^{-1}$	none	yes single probe (uncooled)	yes	>99%	First significant study collecting over 1300 data samples
Lee and Whipple (1981)	0.8 cm dia. Model Flare (unrestricted area 6.5 cm^2)	Commercial grade propane	89	none	10^{-3} - 10^{-4} $m^3 \cdot s^{-1}$	% helium	yes single probe	yes	>99% propane destruction efficiency	Objective to evaluate hydrocarbon destruction in a flare
Remote Sensing EPA ROSE SYSTEM Herget (1977)	Initial tests on full-size flare 1.2 m dia. x 41 m high	Carbon Black Vinyl Monomer	N/A	N/A	N/A	none	remote sensing	none	2500:1 CO reduction	Initial tests compared flare offgas concentrations to concentrations in an unignited flare. Additional tests discussed below.
EPA/Howes (1981)	Zink STF-LH (20 cm dia.) Pilot Air-Assisted Flow	Commercial grade propane	89	Air Flow Classified	1.5-2.2 $t \cdot h^{-1}$	none	yes single probe also remote sensing	yes	>99%	Objective is to establish test procedures for future testing. Remote sensing data (ROSE) inclusive.
	Zink LRGO staged Flare Burner	Natural Gas			1-1.5 t h^{-1}					
CMA/EPA/McDaniel (1983)	Zink STF-S-8 (20 cm dia.) Stream Pilot Flare	Propylene diluted with N_2	7.2-81.3	0-7 and 123	.01-19 $m \cdot s^{-1}$	SO_2 and mercaptan	yes single probe also limited remote sensing	yes	>99%	Tested low flow, low Btu content gases over a wide range of operating conditions - Tracer aspects inconclusive. Remote sensing data being analyzed.
	Zink STF-LH (20 cm dia.) Air-Assist Pilot Flare		3.1-81.3	2 air flow rates	.04-66 $m \cdot s^{-1}$					
EPA/EER/Joseph et al. (1983) 1983 - Continuing	Test model flares 3.8, 7.6 15.2 cm dia.	Commercial grade propane diluted with Nitrogen	11.2-50.3	0-1	.15-3.0 $m \cdot s^{-1}$	SO_2	yes simultaneous 7 probe rake	yes also using hood to capture offgases, and tethered balloon samples	Preliminary >98%	Comprehensive test of scale model flares to evaluate wide range of operating variables - collect data for full-size scaling criteria
	Commercial Flare Tests planned									

released from the side of the flame. Lee proposed that the release of these eddies had the greatest effect on flare efficiency.

EPA ROSE/Herget (1978) Preliminary studies were conducted using the EPA Remote Optical Sensing Equipment (ROSE) to estimate CO emissions from a carbon black flare. Direct evaluations of combustion efficiencies were not made, although ROSE results expressed as a ratio of CO concentrations (without flame/ with flame) showed a 2500:1 reduction.

EPA/Howes (1981) The objective of this test program was to develop and evaluate equipment and methods for emission measurements using extractive sampling techniques. Additional simultaneous measurements were also made using the EPA ROSE. Both methods indicated high combustion efficiencies associated with normal flare operations.

CMA/EPA/McDaniel (1983) The study showed that combustion efficiencies were on average greater than 98 percent for air assisted flares when heat contents of burned gases were greater than 10 $MJ \cdot m^{-3}$. Much lower efficiencies of only about 50 percent were observed for gases with heat contents of about 5 $MJ\ m^{-3}$. Steam assisted flares with steam to burner gas ratios of greater than 3.5 were also found to be inefficient.

EPA/EER/Joseph et al. (1983) This study currently in progress is designed to test pilot flare performance and determine a method of scaling these results to full scale flares.

None of the above studies appear to have had model guidance as to how combustion efficiencies might vary with flare gas parameters and meteorological variables. At present, the only guidance seems to be the assumption that flares will be efficient, providing heat contents of flared gases exceed a specified value. While this is often taken as 7.45 $MJ \cdot m^{-3}$ (Dubnowski and Davis 1983), Alberta Environment prefers a somewhat higher values of 9 $MJ \cdot m^{-3}$. More elaborate theoretical considerations would presumably involve an evaluation of flame shapes, areas, and radiational properties. It is of interest then to consider the literature relating to these properties with the intention of developing a model which might be used to provide guidance as to the most efficient means of conducting combustion research. The model will ideally demonstrate how various stack and meteorological parameters affect flare geometry and hence combustion efficiencies.

There have been very few reported studies which consider the surface areas of jet diffusion flames. Appreciable work has been done however, in the empirical evaluation of shapes and sizes of flames (Brzustowski 1972, 1973; Gollahalli 1977; Gollahalli et al. 1975; Becker and Liang 1978; Steward 1970; Beychok 1979). Much of the work has resulted in methods to predict gross average features of the flame such as the distance of the flame tip to the burner tip. Perhaps the most widely used empirical method for predicting this length is the one proposed by Brzustowski (1972, 1976) which has some theoretical foundation. Its accuracy is to within about a factor two.

Kalghatgi (1983) has published data on wind tunnel studies concerning the shape and size of turbulent hydrocarbon jet diffusion flames in a cross wind. His information is unusually detailed. Empirical curves fitted to his data showed that both flame heights (h_f) and angles of the flame to the vertical (α_B) were apparently functions only of the ratio of wind speed to stack exit speed (R). (Plume parameters h_f and α_B are illustrated in Figure 1). His derived empirical relations which force fitted data with correlation coefficients of 0.99 are as follows:

$$h_f/D_o = (m_o/m)^{\frac{1}{2}} (6 + 2.35/R + 20R); \text{ and} \tag{2}$$

$$\alpha_B = 94 - (1.6/R) - 35R; \tag{3}$$

where m_o, m = molecular weights of air and flare gas, respectively; and

D_o = stack diameter.

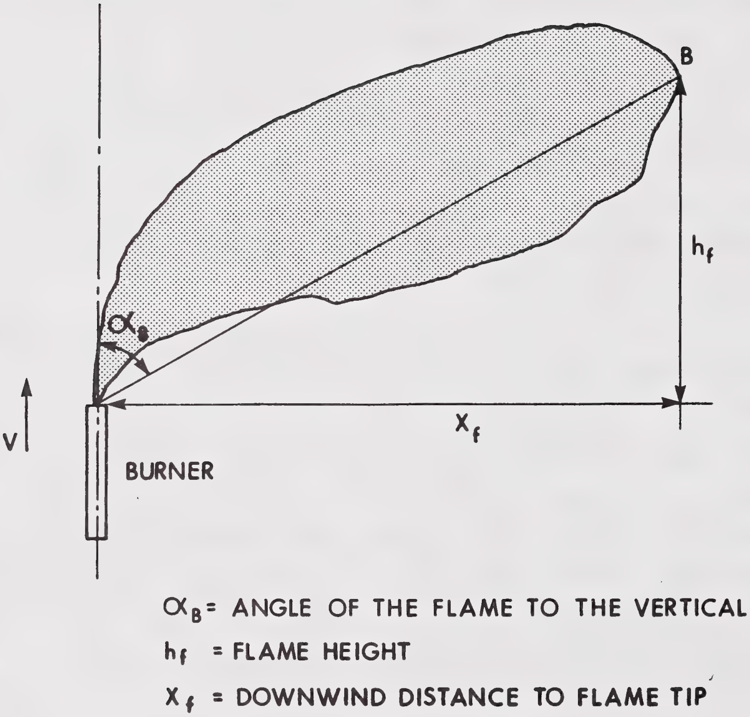
B
h_f
α_B
V
X_f
BURNER
α_B = ANGLE OF THE FLAME TO THE VERTICAL
h_f = FLAME HEIGHT
X_f = DOWNWIND DISTANCE TO FLAME TIP

Figure 1. Sketch of the Flame, Showing Plume Parameters Indicated by Kalghatgi (1983).

Agreement between Kalghatgi's wind tunnel data and predictions using Brzustowski's empirical relationships was very poor. Further work by Kalghatgi indicates that flame shapes associated with industrial flares are not well predicted by equations (2) and (3).

There have also been attempts to develop theoretical models of diffusion flames. Numerical solutions of detailed differential equations which describe the flow have many drawbacks due to difficulties in modelling chemical reactions, turbulent flow fields, and requirements for large computer storage. Attempts have also been made to model the diffusion flame employing theories developed for buoyant chimney plumes (Escudier 1972; Brzustowski 1977). Escudier's calculations which considered chemical reactions are important because they showed that plume behaviour tends to be governed by momentum and be independent of buoyancy and thermal radiation. There was no comparison, however, between model results and observations. Brzustowski's model assumes top hat profiles for velocity, composition and temperature within the diffusion flame. Chemical reactions and separate equations for vertical and horizontal momentum were considered. Evaluation of model results showed large discrepancies between predicted and observed flame lengths.

Parameters relating to jet diffusion flames such as rates of entrainment, flame temperature and radiation effects have been evaluated observationally by many authors.

Both experimental evidence (Ricou and Spalding 1961) and theory (Morton 1965; Townsend 1966) show that the rate of entrainment β for a jet whose density ρ is different from that of the surroundings (ρ_o) is given by:

$$\beta = \beta_o \left[\frac{\rho}{\rho_o}\right]^{\frac{1}{2}} \quad ; \qquad (4)$$

where β_o is the entrainment constant for a jet of density ρ_o.

Temperatures associated with the combustion of hydrocarbons such as methane, propane or butane are usually observed to be about 1900°C (Lewis and Von Elbe 1961). These values however, are not relevant to flare flames which are subjected to greater cooling effects of wind and radiation than are furnace fires. Theoretical considerations show that comparable hydrocarbon flare temperatures may be as low as 1100°C (Masliyah and Steward 1969; Beychok 1979). Detailed measurements in a laboratory of temperatures associated with a propane flame in calm winds and low exit velocities showed them to be about 1000°C (Brzustowski et al. 1975). These were observed to increase to 1200°C as wind speeds and exit velocities increased. Studies of an industrial flare at moderately high wind speeds have shown temperatures between 1150 and 1550°C (Leahey and Davies 1984).

The fraction of heat release F which is radiated from a flare has classically been assumed to be a function only of the molecular weight of the consumed gas (Zabetakis and Burgess 1961; Hajek and Ludwig 1960; Kent 1964; Tan 1967; Oenbring and Sifferman 1980). The highest values cited are those of Oenbring and Sifferman who recommend using a value of 0.25 for light gases and 0.50 for heavy gases. Measurements of radiation from an industrial flare burning a mixture of hydrocarbons, hydrogen sulphide and fuel oil gave average F values of about 0.55 (Leahey and Davies 1984). Studies by Brzustowski et al. (1975) showed that F was not a constant but had a tendency to vary with wind speed.

None of the above studies give models which can be used to assess flare efficiencies in terms of stack and meteorological parameters. A model will be developed later in this report for estimating the length, shape and area of diffusion flames. The model, which can be further developed for predicting flare efficiencies promises to supply necessary guidance regarding flare behaviour.

2. FIELD STUDY

Evaluations of flaring activity were made 6, 7, and 8 March 1984 at a gas plant operated by I.C.G. Resources Ltd. at Acheson, situated about 12 km west of Edmonton. The facility has a 24 m flare stack with a 10 cm diameter. The stack nozzle is surrounded by three pilot lights which are used to maintain a flame.

2.1 MATERIALS AND METHODS

Flare feed streams and combustion plumes were analyzed for a wide range of gases including mercaptans. Flare feed streams were additionally analyzed for trace elements. Interviews of sour gas plant operators were conducted as part of an overall study to assess flaring activity in Alberta.

2.1.1 Flare Feed Stream Compositions

The compositions of the flare feed streams were determined by gas chromatography. Grab samples were taken by drawing the gas through P_2O_5 (fine powder) into glass sample envelopes. These samples were then analyzed on site with a Hewlett Packard 5880A Gas Chromatograph employing molecular sieve 5A and specially treated Porapak QS columns for separation and two different detectors. The Hewlett Packard single-filament thermal conductivity detector was used for the following components: H_2, Ar, O_2, N_2, CH_4, CO, CO_2, C_2H_6, H_2S, COS, CS_2, C_3H_8, C_4H_{10}, C_5H_{12}, C_6H_{14}, $C_7H_{16}+$, C_2H_4 and C_2H_2. An HNU Systems Inc. Model PI-52-02 photoionization detector with a 10.2 eV lamp was used for CH_3SH, C_2H_5SH, C_3H_7SH, C_4H_9SH, $(CH_3)_2S$ and CH_3SSCH_3.

Gas chromatography was chosen as the analytical method because it is the only method capable of conveniently yielding multicomponent analyses with a reasonable degree of accuracy on each component. The two key steps in applying the method are selection of the column packing material to effect the component separations and selection of an appropriate device for detecting and quantifying the components. Both steps are empirical. A complete discussion of the gas chromatographic method is beyond the scope of this report. However, some key aspects are noted.

While many column packing materials are available, the actual selection for a particular application can be very tedious. The key criteria, assuming component separation is achieved, is that the material cannot react with the sample components nor can it be catalytic towards reactions among sample components. The thermal conductivity detector is a universal detector because it will respond to the presence of any gas that changes the thermal conductivity relative to the pure carrier gas. The photoionization detector is a selective detector because it generally responds only to compounds having ionization potentials lower than the excitation energy of the light source.

The molecular sieve 5A column (80/100 mesh, 6 ft x 1/8 in outer diameter (O.D.), stainless steel) and thermal conductivity detector were used to determine H_2, Ar, O_2, N_2, CH_4 and CO. The remaining components have such long retention times on this column that for the purpose of the analysis, they are effectively "absorbed" by the column. The chromatograph operating conditions were: (1) He flow at 30 mL/min; (2) injection port at 125°C; (3) oven at 100°C (isothermal); and (4) detector block at 125°C.

The components separated by the molecular sieve 5A elute as a single peak on the Porapak QS column (80/100 mesh, 6 ft x 1/8 O.D., stainless steel). This was used to separate the rest of the listed components. The photoionization detector was operated at 150°C. In addition, oven temperature were programmed to begin at 45°C for 1 min, increase at 10°C/min to 160°C, hold for 5.0 min, increase at 20°C/min to 200°C and hold finally for a maximum of 10 min. Representative chromatographs are reproduced in Appendix A, along with the results of field calibration checks for the two detectors.

The accuracies of the results obtained by the chromatographic method are dependent upon many factors and, again, a thorough discussion is beyond the scope of this work. In general, the uncertainty on the result increases as the concentration of the component decreases. For routine analyzes, the uncertainties on major and intermediate components (5 to 100 mole percent) can be held to within 1 to 3 percent of value or better. For minor components (1 to 5 mole percent), the uncertainties increase to 5 to 10 percent of the value. For lesser components, the uncertainties increase rapidly and approach (often exceeding) 100 percent of the value at the lower detection limit.

Hewlett Packard specification for the thermoconductivity detector sensitivity is a minimum detectable limit of 4 x 10^{-10} g/mL for C_3H_8. Western Research experience indicates the practical minimum detectable limit for the sulphur gases is about 5 ppm with a ½ mL sample size. The sensitivity of the photoionization detector is a minimum detectable limit of 2 pg of benzene. Western Research experience indicates a minimum detectable limit of 1 ppm for the mercaptans and disulphides when using a 1 mL sample size. The linear dynamic range of the detector is greater than 10^7.

Trace element (metal) contents of the flare feed streams (acid gas and fuel gas) were determined by a chemical absorption system. This system, depicted in Figure 2, was originally devised in collaboration with the Pollution Control Laboratory in Edmonton for preliminary sampling of sulphur plant incinerator stack gases (Paskall 1974). The method since then has not been further refined or tested with respect to collection efficiency or absorbing solution composition. It was used here because the intent was to obtain preliminary estimates of the trace elements and a standardized procedure was not available. Since it is difficult to evaluate and compare data obtained by diverse methods, a standardized method is required if emphasis on trace element (metal) emissions continues.

All parts of the sampling train that contacted the gas sample were Teflon and Pyrex glass, and in preparation for a run, all were washed with reagent grade 0.1 N HNO_3. The Teflon probe extended into the gas stream through a sampling valve; the impinger size was 250 mL.

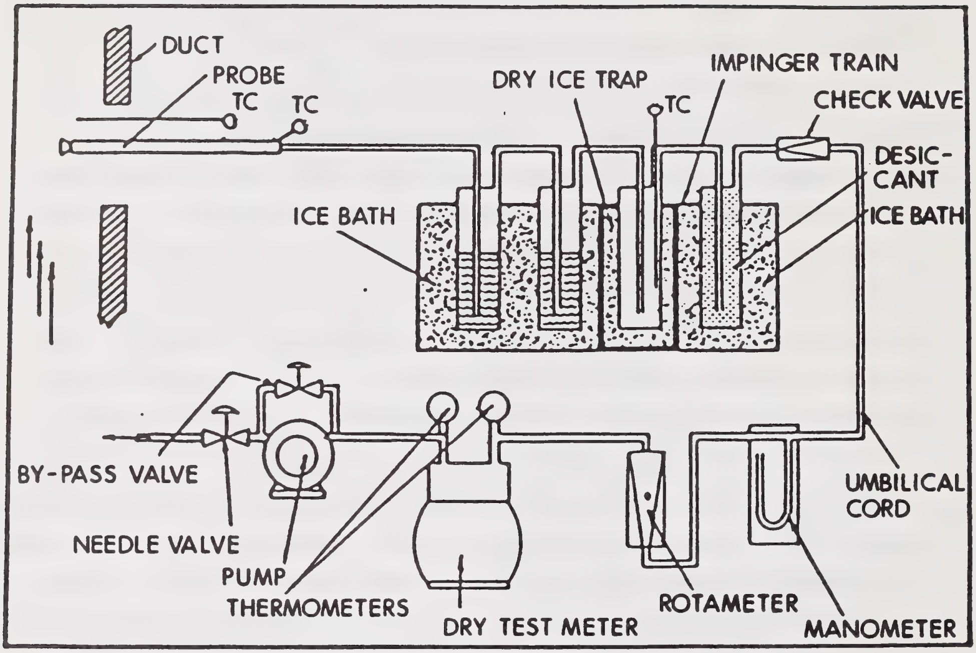

Figure 2. System for Determining Trace Species (Heavy Metals) (Paskall 1974).

For sampling the fuel gas stream, the first two impingers (packed in ordinary ice) each contained 100.0 mL of 0.2 N HNO_3 and the third impinger (packed in dry ice) was left dry. For sampling the acid gas stream, a fourth impinger (packed in ordinary ice) was added between the dry impinger and the desiccant. This impinger contained a saturated solution of NaOH to scrub the H_2S, thereby, protecting the dry gas meter, pump and operator.

Before and after each run, the sampling train was pressure tested to assure that all connections were gas-tight. Three one-hour absorptions were run on each stream; the sampling train parameters were monitored and recorded at regular intervals.

After a run, solutions from the first two impingers were combined with the liquid (melted ice) from the third impinger and the total volume measured to determine the water condensed from the gas stream. The probe and first three impingers were then washed with 50.0 mL of 0.1 N HNO_3 and the washings combined with the impinger solutions. The samples were stored in Pyrex glass bottles and transported next day to Metro-Tech Systems Ltd. in Calgary for metal analyses. A reagent blank containing 200.0 mL of absorbing solution plus 50.0 mL of wash solution was included for analysis. Only one reagent blank was required because all absorbing solutions and wash solutions were prepared from the same batch of stock reagents.

Except for Hg, the metal analyses were carried out on an Inductive Coupled Argon Plasma Spectrometer, with special precautions to assure absence of interferences for Pb, Cd, As and Se. Each sample was analyzed in duplicate which were required to agree within ±10 percent for acceptance of the analysis. Atomic absorption (with internal blank compensation) was used to determine Hg. Both instruments were calibrated with certified standards.

2.1.1.1 Sampling Complications. In every case, there was significant build up of ice on the down-comer of the dry impinger, which restricted gas flow. In the first test on each stream the flow had practically stopped at the end of the test. For the first acid gas run, this flow restriction resulted in backflow of NaOH into the third impinger during the pressure test at the end of the run. This contaminated the melt collected during the test. The whole contaminated solution in this impinger was discarded (which accounts for the lower total volume for this run). The impinger was washed for the next runs. These next two runs exhibited high Na levels due to insufficient washing of the impinger. Since the contaminated impinger was also used for the runs on the fuel gas, the Na indicated for the fuel gas were also treated as contamination.

In the first run on the fuel gas, a slight leak on the second impinger gasket developed sometime during the last 10 minutes of the test as the flow restriction increased due to ice buildup in the third impinger. No condensation of hydrocarbon in the dry ice impinger was achieved or expected since all stream components have melting points lower than that of dry ice and less than 3 percent of the stream components have boiling points greater than dry ice temperature.

Following field work, the dry gas meter was recalibrated against a wet test meter maintained in the laboratory for this purpose.

To compute concentrations of metal species in the acid gas stream, dry gas metered during each test had to be corrected for the H_2S and CO_2 scrubbed by the NaOH, CO_2 removed by the dry ice impinger and for the H_2O condensed in the first three impingers. Measured increase in solution volume and the H_2S and CO_2 concentrations obtained from the gas chromatograph analyses of the stream were used to perform these corrections. These calculations were straightforward and therefore are not detailed here. It was assumed, the gases behaved ideally which is reasonable for the temperatures and pressures that were obtained during the tests. (The H_2O concentration for run 1 was assumed as the measured average values from runs 2 and 3).

2.1.2 Plume Sampling

Sampling of the flare plume was accomplished by using a crane to suspend a basket near the top of the flare stack. Two men in the basket were able to obtain samples from various locations in the flare plume using a high volume sampling technique (Kerr et al. 1975) summarized in Figure 3. The chief criteria of this system are that residence time in the probe (Vycor liner in a steel sheath) be minimized to quench any ongoing reactions and that the construction materials not interact with any of the stream components. A slipstream technique is used to draw a dried portion of the stack gas stream into the glass sample envelope. A tee/pinch clamp arrangement facilitates the elimination of air from the system by purging with stack gas just prior to obtaining the sample. All sample envelopes are filled with He prior to sampling to exclude air and reduce purge time. After sampling, the sample pressure is immediately adjusted to about 35 kPa above atmosphere with a regulated He supply.

The desiccant employed for drying the samples was P_2O_5 powder. This was shown empirically by Western Research (Ca 1971) to be the preferred desiccant for sampling sulphur plant process streams. There was no detectable adsorption of sulphur gas components and the P_2O_5 did not catalyze reactions among the sulphur gases. H_2O removal was effected above the H_2O dewpoint temperature.

Empirical checks were conducted as required while sampling streams with lower concentrations but more components. This ensured no adverse effects on sample integrity.

The glass sample envelope was Pyrex glass, with ground glass stopcocks, very sparingly lubricated with silicone stopcock grease. The rubber serum cap was covered with Teflon tape to eliminate absorption of sulphur gases. No attempts were made to passivate the glass surfaces.

The plume samples obtained were effectively "spot" or instantaneous samples - i.e. drawn quickly from a fixed (?) point in the plume - as opposed to time or space integrated samples. The

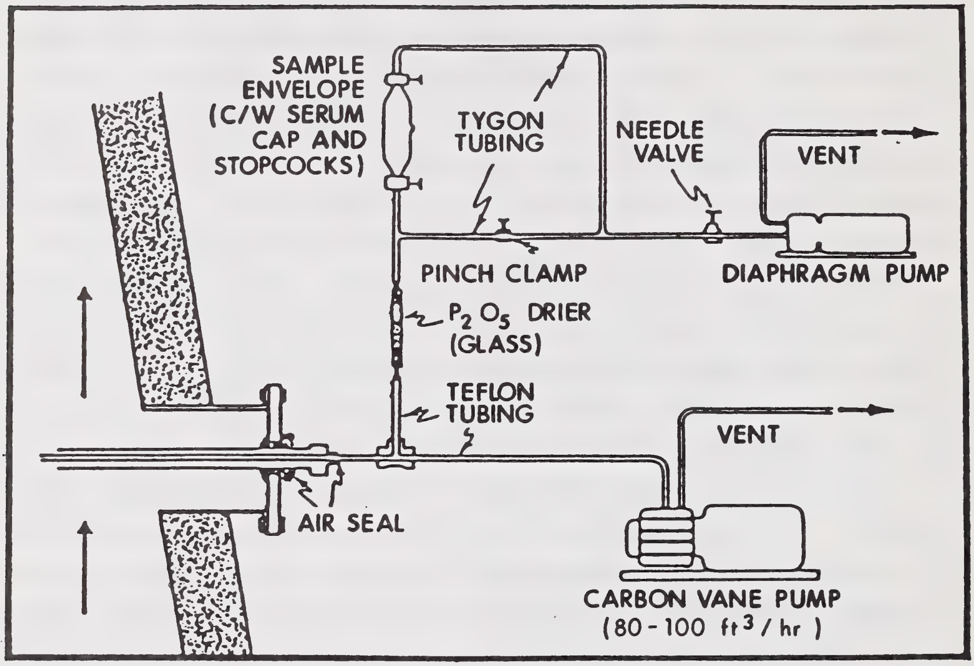

Figure 3. System for Determining Trace Reactive Gas Streams (High Volume Sampler Method). (Kerr et al. 1975)

reason for this is two-fold. Firstly, since detection of unoxidized sulphur gases was an objective, rapid sampling was necessary to quench reactions by quickly cooling the gases. This was also the reason for using the slip-stream sampling technique (Kerr et al., 1975). Secondly, it was not considered practical to attempt integration of the sample over time or space because of the difficulties encountered in defining the location of the flame, especially under the less than ideal conditions of the sampling technique.

Two-way radio communication was maintained during sampling between the crane operator and the samplers for the purposes of positioning the basket. The flare burned with a barely visible flame. Therefore, wind direction and temperature at the probe tip had to be used for positioning the probe within the plume. For this purpose a thermocouple was included in the probe bundle. The probe itself was a 1 m length of 6 mm Vycor glass connected to sampling pumps by 3.52 m of 6 mm Teflon tubing. Mechanical support for the probe and thermocouple was provided by a 3.7 m length of aluminum channel. Use of the thermocouple ensured that plume sampling extended beyond the flame tip. Plume samples were analyzed under the same chromatographic conditions as the flare feed stream samples.

Flame temperatures were measured using a Mikron Model 52 infrared thermometer. This instrument is designed to measure the temperature of flames and hot gas mixtures containing CO_2. It features a narrow band-pass filter centred on 4.5 microns that permits accurate flame temperature measurements which are not affected by cold CO_2 or other normal atmospheric gases. A 30 cm path through a clean flame achieves an emissivity of nearly unity at 4.5 microns. Maximum flame temperatures were observed to rapidly decrease from about 2000 to 1500 K as measuring distances increased from 3 to 15 m, respectively. Temperatures tended to stabilize at about 1300 K at measuring distances beyond 40 m. This tendency for higher temperatures to be observed at closer measuring distances was ascribed to local hot spots which would have greatest influence on temperatures measured close to the flare where the field of view is restricted.

Measurements of wind velocity required for analyzing flare behaviour were made with a wind anemometer attached to a 2.7 m boom located 2.5 m below the flare stack exit.

For safety reasons testing of flare gas compositions was only performed during the day. As stated previously, the flame was difficult to see at this time. Flame dimensions were obtained from photographs taken with 5 second exposures during evening hours when the flare was visible. These photographs were interpreted to give flame rise and length according to a well known technique described by Halitsky (1961). Surface areas were obtained by generating a surface of revolution by rotating the cross-sectional areas about the plume axis. This approach consists mathematically of multiplying the cross-sectional area by π.

2.1.2.1 Sampling Complications. For a number of samples, an unexpected interference with the C_2H_5SH analysis was encountered. A very large peak with a retention time just slightly greater than C_2H_5SH appeared, and overshadowed any C_2H_5SH peak. This peak was subsequently identified as acetone, which had been used earlier to clean the glass sampling envelopes. Following this discovery, after test No.4, a blank run was done on each glass envelope used for plume sampling to assure the acetone had been removed. Test 2 C_2H_5SH data should be considered of questionable value.

2.1.3 Interviews of Sour Gas Plant Operators

Interviews were conducted with operators of nine gas plants in Alberta for purposes of ascertaining the manner in which the volume and compositions of flared gases are monitored. Questions were also asked regarding monitoring of the flame itself.

Efforts were made to select plants which were representative of small, medium and large size facilities. Selections were made in concert with Alberta Environment personnel.

Six of the interviews were conducted by telephone while the remaining three were conducted at the plant site. The questionnaire used for guidance in the interview is contained in Appendix B.

2.1.4 Model Development

Observations of flare behaviour at Acheson relating to flare combustion efficiency were of a preliminary and limited nature. It was not possible to evaluate effects of widely varying wind speeds, exit speeds and fuel compositions. It will be difficult to deduce the general behaviour of flares solely on the basis of these particular observations.

However, Acheson data could be used to assess predictions of a model, derived from physical laws, which describes relationships between flare combustion efficiency, meteorology and stack exit parameters. The model should ideally provide reasonable explanations for the observed Acheson data. If this is the case then a basis might be established for generalizing about flare behaviour at other locations in Alberta and elsewhere.

The manner in which a flare efficiency model may be derived is indicated in this report. Steps have been taken, as part of this study, towards a model development. Though not fully completed, the model does provide insights into flare behaviour which are in general agreement with observations.

3. RESULTS AND DISCUSSION

Compositions of the Acheson flare gas stream and flare plume were assessed with respect to combustion efficiencies and the presence of heavy metals and mercaptans. Responses of sour gas plant operators to interviews regarding flaring activity were summarized. The manner in which a model for flare efficiency might by developed was postulated and partially tested.

3.1 FLARE FEED STREAM EVALUATIONS

Equipment assembly and preliminary flame observations were conducted on March 6 to finalize sampling and testing procedures. Tests were undertaken on March 7 and 8, 1984 for purposes of assessing flare efficiencies.

Table 2 presents times, flame temperatures, heat content of flared gases, stoichiometric mixing ratios, exit speeds and wind velocities for all tests conducted on 7 and 8 March. Stack exit speeds were determined by measuring the volumes of gas going to the flare stack. Net heat contents and mixing ratios were calculated from gas composition data. Different flare gas flow rates were achieved by altering the amounts of fuel gas added to the plant acid gas. Analyses of fuel and acid gases for March 6 and 8 are given in Table 3. Compositions tended to remain constant.

Flare gas analyses obtained following mixing of the fuel and acid gases for all daytime tests are shown in Table 4. Parameters relating to net heat content and mixing ratios shown in Table 1 for evening hours were obtained by measuring flow rates and assuming that acid and fuel gas compositions were the same as those shown in Table 3.

Concentrations of mercaptans, dimethyl sulphide and dimethyl disulphide as observed in the acid and fuel gas streams are shown in Table 5. Detection levels were about 1 ppm. Methyl, ethyl and propyl mercaptans were detected in the acid gas at concentrations in the order of 100 ppm. None of the chemicals were detected in the fuel gas.

Table 2. Flare Stack Parameters for Indicated Test Times.

Test	Time (MST)	Flame Temperature (K)	Heat Content ($MJ\cdot m^{-3}$)	Mixing Ratio (%)	Exit Speed ($m\cdot s^{-1}$)	Wind Speed ($m\cdot s^{-1}$)
March 7						
1	12:32-12:42	1373	16.8	16.7	7.2	6.1
2	14:28-14:31	1153	11.5	22.4	5.9	4.4
3	15:48-15:57	1313	13.3	20.1	6.4	3.2
4	20:02-20:04	1353	17.6	16.1	7.6	1.3
5	20:16-20:18	1323	15.5	17.8	7.1	1.4
6	20:33-20:34	1213	12.5	21.1	6.1	1.4
7	21:01-21:03	1273	13.4	20.0	6.3	1.3
8	21:03-21:04	ND[a]	13.4	20.0	6.3	1.1
March 8						
9	10:23-10:35	1283	16.2	15.4	7.7	1.6
10	12:39-12:48	1313	11.9	21.9	6.7	1.4
11	13:52-14:01	973	7.9	29.1	5.7	1.1
12	21:23-21:24	1203	4.1	42.6	5.0	2.8
13	21:50-21:51	1273	18.6	15.4	8.5	2.8
14	21:56-21:57	1103	14.0	19.3	6.7	3.2
15	22:07-22:08	1073	10.7	23.7	5.8	3.0
16	22:25-22:26	673	4.1	42.6	4.6	3.2
17	22:33-22:34	823	8.1	28.7	5.3	2.8

[a] ND = No Data

Table 3. Compositions of Acid and Fuel Gases for the Indicated Periods (Mole Percent on Dry Basis).

Component	Acid Gas			Fuel Gas	
	09:54 March 6	14:38 March 6	09:12 March 8	10:19 March 6	09:20 March 8
H_2	0.000	0.000	0.000	0.000	0.000
Ar	0.000	0.000	0.000	0.000	0.000
O_2	0.000	0.000	0.000	0.000	0.000
N_2	0.043	0.010	0.421	4.725	3.992
C_1	1.412	0.793	1.805	73.247	74.465
CO	0.000	0.000	0.000	0.000	0.000
CO_2	83.997	85.427	83.203	0.010	0.011
C_2	0.394	0.214	0.486	19.303	19.221
H_2S	13.623	13.299	13.554	0.000	0.000
COS	0.000	0.000	0.000	0.000	0.000
SO_2	0.000	0.000	0.000	0.000	0.000
CS_2	0.000	0.000	0.000	0.000	0.000
C_2H_4	0.000	0.000	0.000	0.000	0.000
C_2H_2	0.000	0.000	0.000	0.000	0.000
C_3	0.246	0.144	0.343	2.708	2.311
iC_4	0.019	0.013	0.034	0.004	0.000
nC_4	0.065	0.041	0.087	0.001	0.000
iC_5	0.012	0.012	0.017	trace	0.000
nC_5	0.012	0.014	0.022	trace	0.000
C_6	0.065	0.048	0.007	0.002	0.000
C_7+	0.114	0.025	0.021	trace	0.000

Table 4. Flare Gas Analysis (Mole Percent on Dry Basis) for Indicated Test Period.

Component	Test 1	2	3	9	10	11
H_2	0.00	0.00	0.00	0.00	0.00	0.00
Ar	0.00	0.00	0.00	0.00	0.00	0.00
O_2	0.00	0.00	0.00	0.00	0.00	0.00
N_2	2.104	1.04	1.99	1.50	1.02	0.61
C_1	28.69	17.51	21.35	32.81	18.46	9.09
CO	0.00	0.00	0.00	0.00	0.00	0.00
CO_2	52.99	66.04	61.62	49.29	65.23	74.39
C_2	6.74	4.19	4.94	7.80	4.24	2.18
H_2S	8.33	10.46	9.91	7.42	10.24	13.16
COS	0.00	0.00	0.00	0.00	0.00	0.00
CS_2	0.00	0.00	0.00	0.00	0.00	0.00
C_2H_4	0.00	0.00	0.00	0.00	0.00	0.00
C_2H_2	0.00	0.00	0.00	0.00	0.00	0.00
C_3	1.08	0.71	0.86	1.12	0.73	0.47
iC_4	0.01	0.01	0.01	0.01	0.01	0.12
nC_4	0.03	0.03	0.03	0.03	0.03	0.04
iC_5	0.00	0.01	0.01	0.01	0.01	0.01
nC_5	0.01	0.01	0.00	0.01	0.01	0.01
C_6	0.00	0.00	0.02	0.00	0.00	0.01
C_7+	0.02	0.00	0.00	0.01	0.03	0.03

Table 5. Concentrations of Indicated Species in Acid and Fuel Gas (ppm by Volume).

Time:	Acid Gas 09:54 March 6	 14:38 March 6	 09:12 March 8	Fuel Gas 10:19 March 6	 09:20 March 8
Methyl Mercaptan	29	62	34	ND[a]	ND
Ethyl Mercaptan	52	60	16	i[b]	i
Propyl Mercaptan	69	192	176	ND	ND
Butyl Mercaptan	ND	ND	ND	ND	ND
Dimethyl Sulphide	ND	ND	ND	ND	ND
Dimethyl Disulphide	ND	ND	ND	ND	ND

[a] ND = Not detectable - detection limit approximately 1 ppm

[b] i = Acetone contaminated

Table 6 shows trace metal concentrations as observed on March 6. Trace metal concentrations in the absorbing solutions as received from Metro-Tech Systems Ltd. are reproduced in Appendix A. Chemical absorption data are also summarized in Appendix A. Three samples from each of the acid and fuel gas streams were assessed. Detection limits are as indicated in Table 6. Most metals were not detected. Only two metals (P, Zn) had measured concentrations above 100 $\mu g.m^{-3}$. These relatively high P and Zn values occured in only one acid and one fuel gas sample, respectively.

Published concentrations of mercaptans and heavy metals as found in flare gas streams were not found. Results shown in Tables 5 and 6 are, however, in general agreement with as yet unpublished information obtained by the Alberta Energy Resources Conservation Board (Thimm 1984).

3.2 PLUME EVALUATIONS

Table 7 shows results of plume analysis at distances of 0.5, 1.0 and 2.0 m from the flare tip. The flame went out during test 2.

Data in Table 7 were analyzed using equation (1) to determine local combustion efficiency (E) with respect to reduced sulphur species. Values of E are shown in Table 8. This table also presents ratios of C to S atoms which should be essentially constant with a given plume. Its value can therefore serve as an indicator of the integrity of sampling techniques.

Table 8 shows that there was incomplete combustion during tests 1, 10 and 11 at a downwind distance of 2 m from the flare stack. Values of the C/S ratio show that the 100 percent combustion found during test 3 is suspect. Poorest combustion, found during test 11 was associated with a heat content of only 7.9 $MJ.m^{-3}$. It was found that flares from tests 3, 10 and 11 could support a flame only if supplied with a constant source of ignition. Failure to supply this ignition resulted in loss of flame during test 2.

Table 6. Trace Element Determination.

	Acid Gas			Fuel Gas		
	1	2	3	1	2	3
Sample	Concentration ($\mu g \cdot m^{-3}$)[a]					
Volume (m^3)[a]	0.556	0.552	0.523	0.360	0.302	0.199
Ag	[c]<2.0	<2.0	<2.0	<3.0	<4.0	<5.0
Al	<7.0	<8.0	<8.0	<11.0	11.6	<19.0
As	<12.0	<12.0	<13.0	<18.0	<21.0	<31.0
B	<3.0	<3.0	<3.0	<4.0	<4.0	<7.0
Ba	<0.1	<0.1	<0.1	0.4	<0.2	<0.3
Ca	<0.1	<0.1	<0.1	<0.1	<0.2	<0.3
Cd	<0.5	1.0	<0.5	<0.7	<0.8	<1.0
Cr	<2.0	<2.0	<2.0	<3.0	<3.0	<5.0
Cu	<1.0	<1.0	<1.0	45.5	<2.0	<3.0
Fe	<1.0	<1.0	<1.0	18.1	<2.0	<1.0
Hg	0.2	1.7	<0.2	<0.7	0.6	1.3
K	<60.0	<61.0	<65.0	<88.0	<104.0	<160.0
Mg	<0.1	<0.1	<0.1	<0.1	<0.2	<0.3
Mn	<0.2	<0.3	<0.2	<0.4	<0.4	<0.6
Mo	<3.0	<3.0	<3.0	<4.0	<4.0	<6.0
Na	<5.0	b	b	b	b	<13.0
Ni	<3.0	<3.0	<3.0	<4.0	17.4	<8.0
P	<14.0	200.0	0.6	<21.0	<25.0	<38.0
Pb	<10.0	3.9	<10.0	<14.0	<17.0	25.2
Se	<10.0	<10.0	<10.0	<14.0	<17.0	<25.0
Si	<5.0	<5.0	<5.0	<7.0	<8.0	<13.0
Sn	<3.0	<3.0	<3.0	<4.0	<5.0	<8.0
V	<1.0	<1.0	<1.0	<2.0	<2.0	<3.0
Zn	4.2	<1.0	8.3	14.7	5.8	120.0
Be	<0.1	<0.1	<0.2	<0.2	<0.2	<0.4

[a] At 21.1°C and 101.325 kPa, corrected for blank

[b] Indeterminate because of contamination of impinger with NaOH

[c] <x Indicates below minimum detectable limit, x

Table 7. Plume Analysis (Mole Percent on Dry Basis) for Indicated Test Period.

	Test 1			Test 2		
	Distance from Flare Tip (m)					
	0.5	1.0	2.0	0.5	1.0	2.0
H_2	0.000	0.000	0.000	0.207	0.000	
Ar	0.917	0.932	0.935	0.882	0.893	
O_2	8.315	10.839	20.078	10.344	19.287	
N_2	76.647	77.904	78.212	73.778	74.685	
C_1	0.349	0.057	0.012	0.492	0.749	
CO	1.342	0.737	0.000	0.847	0.000	
CO_2	11.203	8.787	0.686	11.917	3.574	FLAME
C_2	0.034	0.007	0.005	0.113	0.231	OUT
H_2S	0.005	0.004	0.003	0.211	0.534	
COS	0.004	0.002	trace	0.002	0.000	
SO_2	1.072	0.701	0.069	1.144	0.000	
CS_2	0.024	0.010	0.000	0.007	0.000	
C_2H_4	0.034	0.015	0.000	0.007	0.000	
C_2H_2	0.049	0.004	trace	0.027	0.000	
C_3	0.005	0.001	0.000	0.022	0.046	

Continued ...

Table 7. Continued.

	Test 3			Test 9		
	Distance from Flare Tip (m)					
	0.5	1.0	2.0	0.5	1.0	2.0
H_2	0.248	0.381	0.000	1.712	0.495	0.000
Ar	0.904	0.889	0.935	0.857	0.922	0.938
O_2	13.757	14.241	20.373	6.548	16.133	18.876
N_2	75.555	74.345	78.137	71.624	77.108	78.441
C_1	0.332	0.463	0.000	1.805	0.267	0.011
CO	0.627	0.809	0.024	3.200	0.994	0.058
CO_2	7.472	7.616	0.227	12.339	3.664	1.542
C_2	0.039	0.077	0.000	0.336	0.028	0.002
H_2S	0.060	0.064	0.000	0.131	0.021	0.000
COS	0.003	0.002	0.000	0.008	0.001	0.000
SO_2	0.871	1.040	0.304	1.078	0.302	0.132
CS_2	0.093	0.011	0.000	0.020	0.008	0.000
C_2H_4	0.012	0.015	0.000	0.089	0.030	0.000
C_2H_2	0.019	0.032	0.000	0.198	0.023	0.000
C_3	0.008	0.015	0.000	0.055	0.004	0.000

Continued ...

Table 7. Concluded.

	Test 10			Test 11		
	Distance from Flare Tip (m)					
	0.5	1.0	2.0	0.5	1.0	2.0
H_2	0.385	0.295	0.000	0.000	0.000	0.000
Ar	0.868	0.893	0.932	0.884	0.933	0.914
O_2	10.584	14.251	19.107	17.615	19.742	19.834
N_2	72.567	74.687	77.921	73.947	78.020	76.416
C_1	0.500	0.411	0.110	0.361	0.069	0.183
CO	1.274	0.720	0.101	0.126	0.000	0.000
CO_2	12.226	7.704	1.604	5.978	1.033	2.242
C_2	0.093	0.070	0.012	0.095	0.014	0.049
H_2S	0.142	0.124	0.022	0.512	0.071	0.271
COS	0.001	0.002	0.000	0.000	0.000	0.000
SO_2	1.288	0.781	0.180	0.450	0.114	0.078
CS_2	0.005	0.006	trace	trace	0.000	0.000
C_2H_4	0.011	0.009	0.001	0.001	0.000	trace
C_2H_2	0.038	0.033	0.006	0.007	0.001	0.001
C_3	0.018	0.014	0.004	0.024	0.003	0.012

Table 8. Values of the Local Combustion Efficiency (E) and C/S Ratios Observed at the Indicated Distance from the Stack.

		Distance from the Stack (m)			
	Test	0.0[a]	0.5	1.0	2.0
1.	E	NA[b]	95.0	96.4	95.8
	C/S	11.8	11.7	13.3	9.8
2.	E	NA	83.4	0.0	g[c]
	C/S	9.0	9.9	9.2	g
3.	E	NA	77.8	92.2	100.0[d]
	C/S	9.7	7.6	8.2	0.8
9.	E	NA	85.8	88.8	100.0
	C/S	13.7	14.9	15.0	12.2
10.	E	NA	89.4	85.0	89.1
	C/S	9.2	10.0	9.9	9.2
11.	E	NA	46.8	61.6	22.3
	C/S	6.8	7.0	6.2	7.3

[a] At flame inlet
[b] NA = Not applicable
[c] g = Flame out
[d] Suspect

As indicated earlier, it is difficult to generalize on reasons for observed combustion efficiencies without the use of a physical model. For this reason, discussion regarding values of E will be postponed until after the model presentation given in Section 3.4.

Table 9 presents results of plume analysis for mercaptans, dimethyl sulphide and dimethyl disulphide. Only methyl, ethyl and propyl mercaptans were detected, doubtlessly because of their presence in the acid gas stream. The last two of these mercaptans were present in concentrations as great as about 25 ppm. Concentrations of methyl mercaptan were much smaller. As expected concentrations in the plume showed a tendency to decrease with increasing distance from the stack.

3.3 INTERVIEWS OF SOUR GAS PLANT OPERATORS

The Alberta Energy Resources Conservation Board (ERCB) requires operators of each sour gas plant to supply monthly reports of amounts of flared H_2S. These reports are based upon estimates of the volume of gas flared together with its H_2S content. The success of flaring operations are usually assessed by the visible presence of a flame.

3.3.1 Measurements of Volume Flow

Volumes of acid gas flowing to flare on a continuous basis are usually measured using orifice meters. These produce a record of static pressure, temperature and pressure drop across the orifice. Measurement accuracy for low pressure acid gas streams is about five percent. At some plants, however, the amount of flared H_2S gas is simply assumed to be equal to the estimated amount of this gas entering the plant from various field wells. Unlike the use of orifice meters on gas flow streams, this approach does not provide a check of the estimated inlet sulphur flow rate.

Table 9. Plume Analysis (ppm by volume).

	Test 1			Test 2		
	Distance from Flare Tip (m)					
	0.5	1.0	2.0	0.5	1.0	2.0
Methyl Mercaptan	ND[a]	ND	ND	1	ND	
Ethyl Mercaptan	i[b]	i	i	13	1	
Propyl Mercaptan	11	2	2	11	14	FLAME OUT
Butyl Mercaptan	ND	ND	ND	ND	ND	ND
Dimethyl Sulphide	ND	ND	ND	ND	ND	
Dimethyl Disulphide	ND	ND	ND	ND	ND	ND

Continued ...

Table 9. Continued.

	Test 3			Test 4		
	Distance from Flare Tip (m)					
	0.5	1.0	2.0	0.5	1.0	2.0
Methyl Mercaptan	ND[a]	ND	ND	1	ND	ND
Ethyl Mercaptan	i[b]	i	i	i	i	i
Propyl Mercaptan	5	7	1	30	8	3
Butyl Mercaptan	ND	ND	ND	ND	ND	ND
Dimethyl Sulphide	ND	ND	ND	ND	ND	ND
Dimethyl Disulphide	ND	ND	ND	ND	ND	ND

Continued ...

Table 9. Concluded.

	Distance from Flare Tip (m)					
	Test 10			Test 11		
	0.5	1.0	2.0	0.5	1.0	2.0
Methyl Mercaptan	1	1	ND[a]	1	ND	ND
Ethyl Mercaptan	20	16	7	2	ND	7
Propyl Mercaptan	9	7	1	10	4	6
Butyl Mercaptan	ND	ND	ND	ND	ND	ND
Dimethyl Sulphide	ND	ND	ND	ND	ND	ND
Dimethyl Disulphide	ND	ND	ND	ND	ND	ND

[a] ND = Not detected, detection limit approximately 1 ppm

[b] i = Acetone interference

Volume addition of fuel gas to the acid streams is always measured by orifice meter. It is maintained at a rate required to have a specified fuel gas to acid gas ratio. This ratio is determined by head office personnel in a manner unknown to the plant operator. Some of those interviewed were unaware of the Alberta Environment requirement that fuel gas to acid gas ratios be such as to keep the heat content of the flared gas from falling below 9 $MJ \cdot m^{-3}$. (Tests at two of three locations visited by Western Research showed that this requirement was not satisfied, perhaps because of the arbitrariness in setting gas flows by the head office personnel.)

Hydrogen sulphide is flared not only through stacks designed for continuous use but also through those designed for emergency events. Volume measurements of gas emitted through an emergency flare stack are usually obtained by a meter designed to measure the maximum expected flow. Low volume flows such as those associated with pressure release valves are not accurately metered. In some cases, for example, a zeroing error of one pen width might imply a flaring rate of 1.3 $m^3.s^{-1}$ (4 MMSCFD) of gas. Appreciable amounts of gas may thus be unknowingly emitted.

3.3.2 Measurements of Composition

Measurements of H_2S contents of gas streams at sour gas plants are usually made routinely on at least a weekly basis. Frequency of analysis can increase to three times a week at larger plants.

Evaluation of H_2S content of gas streams at smaller plants are made using direct inexpensive measuring methods such as Tutweiler absorption, Gas Tech, or Draeger tubes. Outside consultants may be hired to do an accurate gas sample analysis on an annual or semi-annual basis. Gas chromatography may be used at larger gas plants for obtaining more accurate analyses of gas compositions.

3.3.3 Flare Monitoring

The only routinely-applied test of successful flaring is the presence of a flame, usually measured visually. Difficulties can be encountered when gas flames are short (1-2 m), at the top of high stacks, and/or of a blue colour.

Because gas flames are not always visible, thermocouple based systems are sometimes employed to test for flame presence. These detect the flame as a result of its heat release. (At two of three plants visited by Western Research personnel, these systems were installed but inoperative.)

Log books maintained by plant operators indicate those occasions when a lack of a flare flame may cause a plant to shut down. Normally such an event occurs when the flame has been out for more than ten minutes and attempts to restart it have failed. Log books also record all emergency flaring events.

Interviews with plant operators indicate that loss of flames on a flare occur less than once a year. Normally they are easily relit through use of an automatic ignition system or flare pistol.

3.4 MODEL DEVELOPMENT AND TESTING

3.4.1 Theory

A flare in which there is complete combustion consists of a jet diffusion flame of volume V_o. This volume is heated as a result of combustion. A portion of the heat released by combustion is radiated outward. Conservation of heat energy is expressed by the equation:

$$\frac{\pi D_o{}^2 HV}{4} = \int_{V_o} \frac{d(C_p \rho T)}{dt}\, dV_o + \int_A \varepsilon \sigma T^4 dA; \qquad (5)$$

where: D_o = flare stack diameter (m);
H = heat of combustion ($J.m^{-3}$);
V = stack exit speed ($m.s^{-1}$);
C_p = specific heat of combusted gas ($J.kg^{-1}.K^{-1}$);

ρ = density of combusted gas within flare ($kg.m^{-3}$);
t = time (s);
T = temperature of gases in flare (K);
A = plume surface area (m^2);
ε = emissivity;
σ = Stefan-Boltzmann Constant;
($5.67 \times 10^{-8}\ J.m^{-2}.K^{-4}.s^{-1}$).

The time derivative in Equation (5) is taken following the trajectory of a parcel of air as it passes through the flame.

If the flare, for purposes of simplicity, is assumed to be of constant temperature and density, have an emissivity of unity and the heat of combustion is assumed to be released uniformly over the flame, then equation (5) can be rearranged to give:

$$V_o = \frac{\pi D_o^2 HV - 4A\sigma T^4}{4C_p\rho(T-T_o)} \cdot t \; ; \qquad (6)$$

Here t = x_f/U
x_f = downwind extent of the flame
U = horizontal wind speed
T_o = temperature of the gas prior to injection.

Equation (6) demonstrates that successful flaring at a constant temperature depends upon the geometry of the diffusion flame. If the volume is smaller than that given in Equation (6), the combustion is incomplete because some of the flare gases are outside the flame volume. If the volume is larger, the amount of combustion will be insufficient to heat the potential flame volume to combustion temperatures.

Flare efficiency will be postulated to be a function of the ratio V_o'/V_o where V_o' is the actual flame volume. Unfortunately, it is not possible to evaluate this theory directly from observational data because flames were barely visible during efficiency tests made during daylight hours. However, flame dimensions were measured at Acheson during the evenings of March 7 and 8. It is possible to develop a model for predicting flame areas and volumes. This model could be tested against the evening data.

It will be assumed that:

(1) Buoyancy forces within the region of the flame are negligible. This assumption is consistent with the theoretical findings of Escudier (1972).

(2) Gas exits from the flare stack in a series of puffs which follow the same trajectory.

(3) Plumes resulting from integration of the puffs have a "top hat" profile. That is, a variable will have a certain constant value inside the plume, another value outside the plume and a discontinuity at the plume boundary.

(4) Plume diameters are proportional to plume rise.

(5) Combustion will not occur in areas of the plume where fuel concentration is less than the stoichiometric mixing ratio.

(6) Molecular weights of flare gas will be equal to that of air. This assumption is reasonable because of the rapid mixing of flare gases at the stack exit.

(7) Entrainment constant β for the flame will vary according to the relation given in Equation (4).

(8) Entrainment constant β, for a jet with density equal to that of air varies with the following relation as proposed by Briggs (1975);

$$\beta_o = 0.4 + 1.2 R \tag{7}$$

With the above assumptions, it can be shown (see Appendix C) that the height of a flame h_f, its length L_f, the angle it makes with the vertical α_B and its area A are given by the relationships:

$$\frac{h_f}{D_o} = \frac{5}{\beta_o} \left[\frac{1}{kR}\right]^{\frac{1}{2}}; \tag{8}$$

$$x_f/h_f = 33\ R/k; \tag{9}$$

$$L_f = (1089\ (R/k)^2 + 1)^{\frac{1}{2}}\ h_f; \tag{10}$$

$$\alpha_B = 90 - \text{arc tan}\ (0.03\ k/R); \tag{11}$$

$$\begin{aligned} \frac{A}{D_o^{\,2}} = \frac{3\pi}{2} \left[\frac{3}{4}\ \frac{T_o}{T}\right]^{1/3} \Bigg[& \frac{\lambda}{\beta} \left\{\lambda^2 + \frac{(1+\beta)^2}{9} \left[\frac{3}{4}\ \frac{T_o}{T}\right]^{2/3} \frac{1}{R^2}\right\}^{\frac{1}{2}} \\ & + \frac{(1+\beta)^2}{9} \left[\frac{3}{4}\ \frac{T_o}{T}\right]^{2/3} \frac{1}{\beta R^2} \log \Bigg\{ \frac{3}{1+\beta} \left[\frac{4}{3}\ \frac{T}{T_o}\right]^{1/3} \Bigg[\lambda R + \bigg\{ \lambda^2 R^2 \\ & + \frac{(1+\beta)^2}{9} \left[\frac{3}{4}\ \frac{T_o}{T}\right]^{2/3} \bigg\}^{\frac{1}{2}} \Bigg] \Bigg\} \Bigg] ; \end{aligned} \tag{12}$$

where: $k = \dfrac{T_o}{T}\ C_s$; and

$$\lambda = \left[\frac{500}{3}\right]^{2/3} \frac{1}{C_s} \left[\frac{T}{T_o}\right]^{2/3}.$$

Values of R and β_o are not constant but fluctuate rapidly with time. This is because of the turbulent nature of the atmosphere.

Equations (4) and (10) were used to estimate the ratio $A/D_o^{\,2}$ for flares with a temperature T = 1500 K. Values for C_s, T_o, and β_o were assumed to be 5.3 percent, 294 K and 0.6 respectively.

(The value for C_s of 5.3 is about midway between the stoichiometric mixing ratios for propane and ethylene.) Results of equation (12) expressed graphically in Figure 4 indicates that A/D_o^2 decreases rapidly as R increases from 0.01 to about 0.05. It is essentially constant at about 2700 for R values greater than about 0.05 and:

$$A/D_o^2 \cong \frac{3927}{\beta_o \, C_s^2} \left[\frac{T}{T_o}\right]^{3/2}. \qquad (13)$$

Calculations were also performed to determine how A/D_o^2 changed with varying β_o. Results for a flame in which R=0.1 are given in Figure 5. As shown, A/D_o^2 decreases as β_o increases. The range of β_o shown in this figure is typical of turbulent diffusion (Leahey and Davies 1984).

The equation for the volume of the flame in the region where equation (13) applies is:

$$\frac{V_o'}{D_o^3} \cong \frac{7854}{\beta_o \, R^{1/2}} \left[\frac{T}{T_o}\right]^{3/2} \left[\frac{1}{C_s}\right]^{5/2}. \qquad (14)$$

Equations (8), (11) and (12) give the flare rise, angle of the flame to the vertical and flare area, respectively. These relations should be evaluated against observations. If they successfully predict the phenomena, then there is reason for believing that V_o' as given by equation (14) should be indicative of plume volume.

Equation (14) explains the observed behaviour of flame efficiency with steam injection. Injection is often employed at low wind velocities to improve combustion. As the amount of steam injection increases, however, beyond a certain value, efficiency again decreases (changes in flame efficiency are monitored by the presence or absence of smoke). This behaviour is in agreement with Equation (14) which predicts large flame volumes at low wind

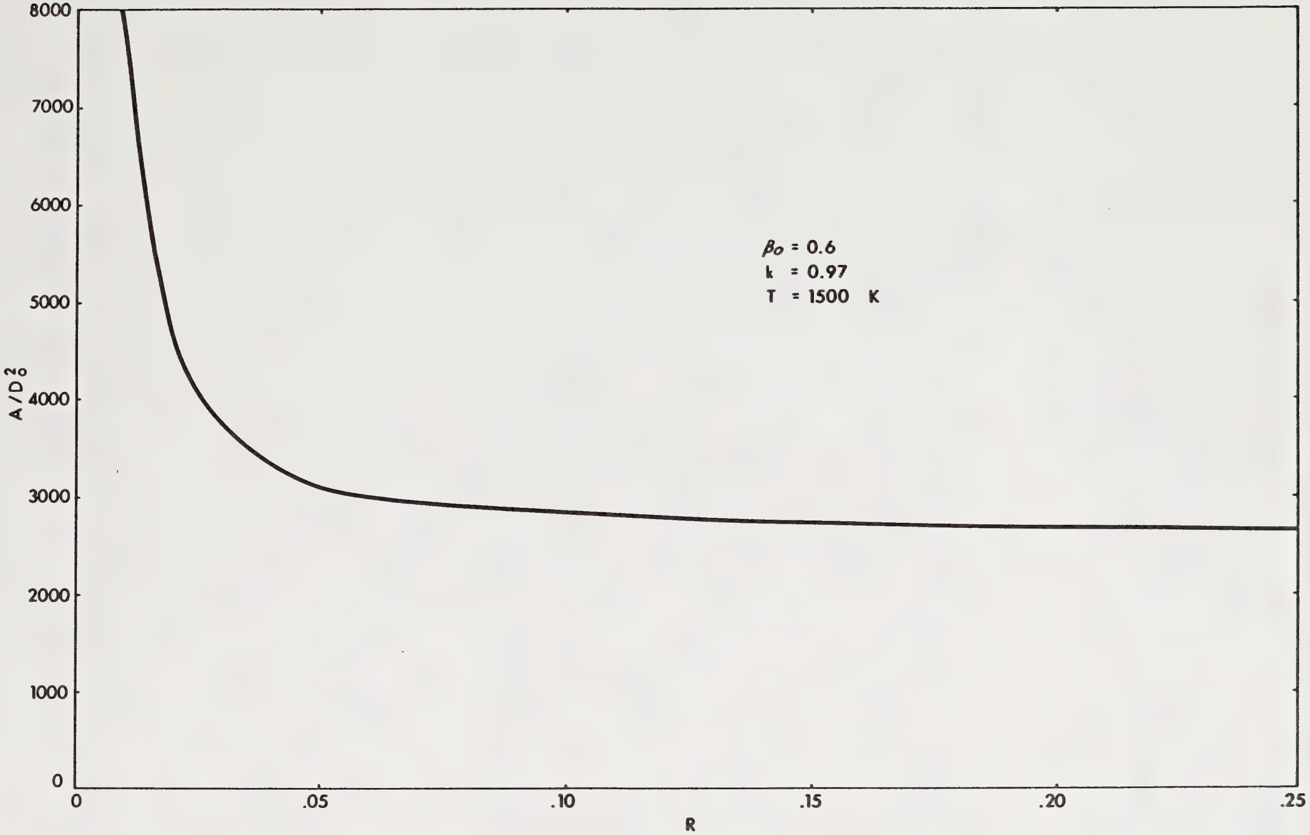

Figure 4. Variation with R of the Ratio of Flame Area to the Square of the Stack Diameter (Equation 12).

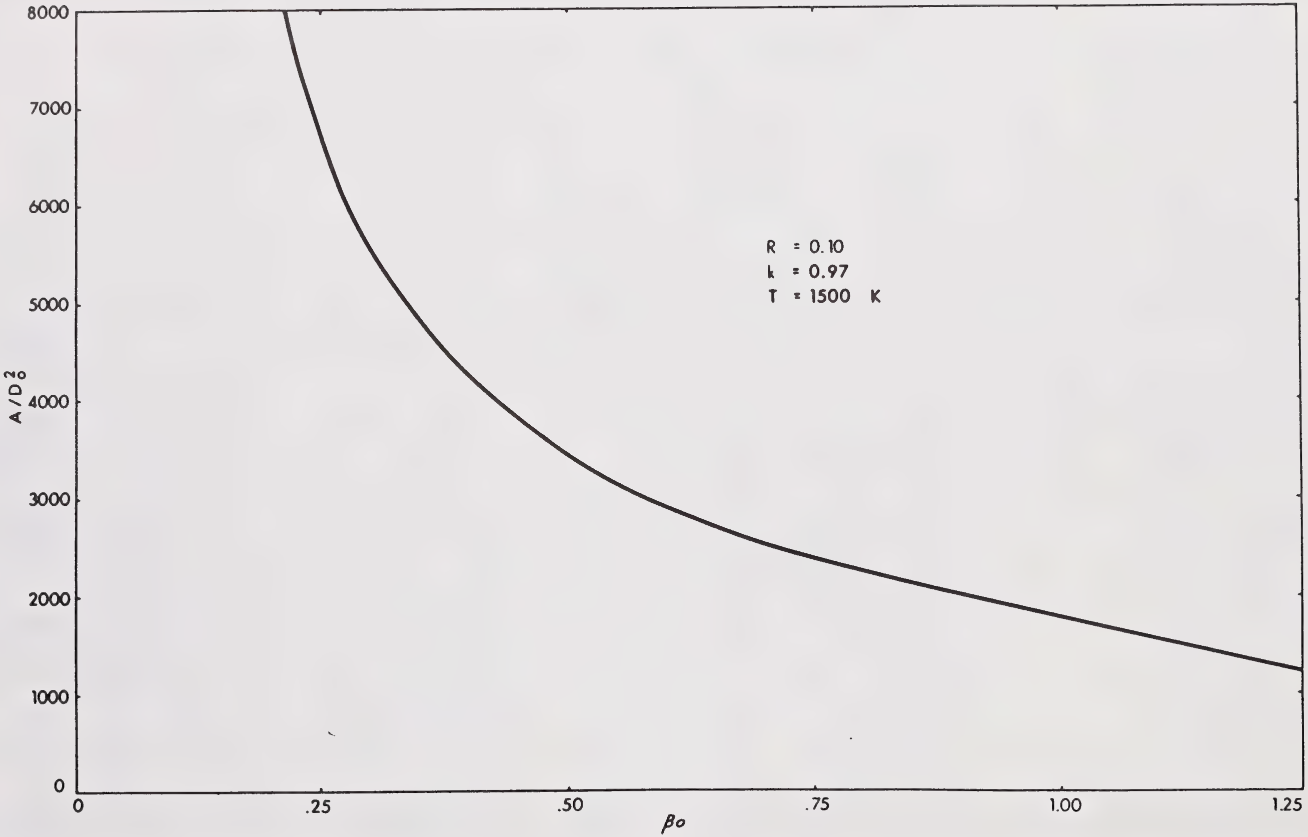

Figure 5. Variation with β_0 of the Ratio of Flame Area to the Square of the Stack Diameter (Equation 11).

speeds (i.e. small values of R). The large volumes are too great to be effectively heated to flame temperature by the available heat of combustion. Steam injection increases air entrainment (i.e. β_o) thus reducing flame volume to a limit consistent with the maximum amount of heat release and required flame temperature. As the rate of steam injection increases the flame volume becomes smaller than that needed to utilize all the potential heat release and flame efficiency again decreases.

3.4.2. Model Evaluation

The theory for diffusion flames described in equations (1) through (12) was tested against wind tunnel data published by Kalghatgi (1983) as well as with data collected at Acheson.

3.4.2.1 Wind Tunnel Tests. Kalghatgi's data relate to the size of hydrocarbon (methane, propane, ethylene, butane) jet diffusion flames. His observations were made using small burners located in a wind tunnel belonging to Sheffield University. The test section of the wind tunnel was 2.65 m high and 2 m wide. Table 10 shows the range of conditions Kalghatgi considered for the indicated gases. The molecular weight, stoichiometric mixing ratio and heat contents of his various gases as obtained from standard handbooks are presented in Table 11.

Kalghatgi presents normalized flame heights as a function of R. He also shows variations with R and the angle α_B between the burner axis and the line joining the tip of the burner to the tip of the flame (Figure 1). All data used in the analysis resulted from averages of five randomly selected observations of the fluctuating flames.

Kalghatgi's normalized height was h_f/D_s where:

$$D_s = (m_o/m)^{\frac{1}{2}} \cdot D_o;$$

m_o, m = molecular weight of air and burner gas, respectively.

Table 10. Range of Conditions Considered by Kalghatgi (1983).

Gas	Burner Diameter (mm)	Range of V Considered (m/s)	Range of U Considered (m/s)	Number of Experiments
Methane	22	35, 44, 52	2.8	3
	14	52, 70, 88	2.8, 3.5	3
	10	150, 108, 52	2.6, 4.7	3
Propane	22	15, 20, 28	2.8, 3.8, 4.5	6
	14	22-56	2.8-5.9	10
	10	48-93	3.3-7.5	14
	6	34-200	2.9-6.9	19
Ethylene	22	14, 28	3.1	2
	14	14-58	3.1, 8.1	8
	10	14-80	3.1, 6	15
	6	29-210	3.1, 6, 8.1	12
Commercial butanes (mol. wt. = 54)	22	13	3	1
	14	21	3	1
	10	21, 34	3	2
	6	21-53	3	4

Table 11. Values of Molecular Weight, Stoichiometric Mixing Ratio, and Heating Contents for the Indicated Gases.

Gas	Molecular Weight	Mixing Ratio (percent by volume)	Net Heat Content[a] ($MJ.m^{-3}$)
Methane	16	9.5	34.0
Propane	44	4.0	88.8
Ethylene	28	6.5	56.0
Commercial Butane	54	3.1	116.2

[a] at 15.6°C and 101.3 kPa

The wind tunnel data were replotted as h_f/D_o, rather than h_f/D_s, and compared to predictions made from Equations (8) and (11).

Values of T associated with the various gases were not available from the literature. A constant value of 1500 K was assumed for evaluation purposes. This is about the average value observed by Brzustowski et al. (1975) during measurements made of a propane flame located in a laboratory. Ambient temperatures were assumed to be 21°C.

Table 12 presents a comparison between predicted and observed values of h_f/D_o. The values of the one-to-one correlation coefficient r shown in the table were calculated according to the relation:

$$r^2 = 1 - \frac{SE^2}{\sigma^2} \; ; \tag{15}$$

where: σ = standard deviation of sample; and

SE = standard error of estimate.

The agreement between average predicted and observed values was good for all gases except methane and butane. The low molecular weight of methane compared to air led to appreciably greater plume rise than predicted. This result was expected as the theory was developed for momentum jets of negligible buoyancy. While agreement between average predicted and observed values of h_f/D_o for butane was good the correlation coefficient was zero. This may be due to the small range of observed values. More observations are desirable in order to better test the theory.

Figure 6 shows the comparison between predicted and observed normalized plume rises for all gases except methane. The solid line is the theoretical one to one relationship. Most of the departures from the line could be explained as due to uncertainties in estimating β_o and/or T.

Table 12. Comparison between Predicted and Observed Values of h_f/D_o for Indicated Gases.

	n	Average Observed h_f/D_o	σ	Average Predicted h_f/D_o	SE	r
Methane	8	76.0	18.0	40.9	36.4	0.00
Butane	8	29.0	9.8	39.0	11.0	0.00
Ethylene	33	37.0	16.5	28.0	10.2	0.79
Propane	52	42.6	17.7	48.3	6.6	0.93
All Gases Except Methane	93	39.1	17.3	40.3	8.5	0.87

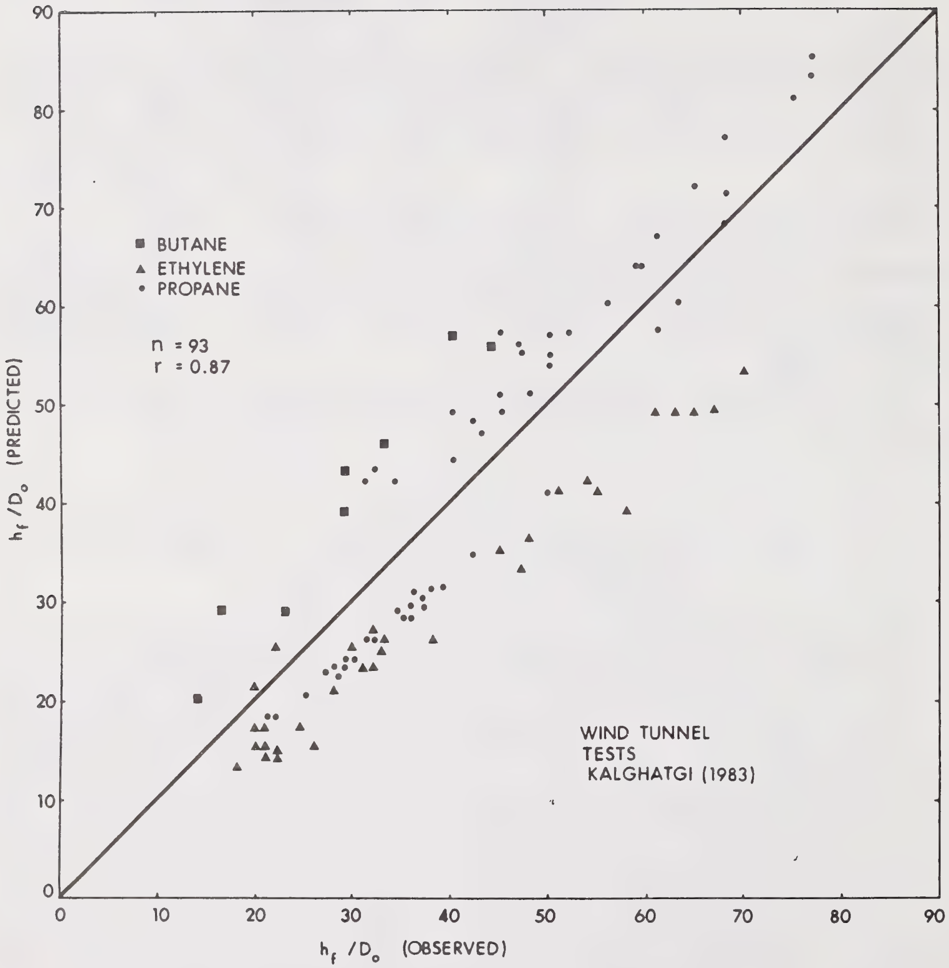

Figure 6. Comparison Between Predicted and Observed Values of h_f/D_o (Wind Tunnel Tests). (Kalghatgi 1983).

Table 13 gives a comparison between predicted and observed values of α_B. Once again the agreement is substantial for all gases except methane. This agreement is shown in greater detail in Figure 7.

3.4.2.2 Acheson Data. Predictions of flare parameters depend upon estimates of its temperature. Flare temperatures as measured by the infrared thermometer varied with its distance from the flame. Because of the uncertainty of temperature values it was decided to assume that the temperatures of all flames as 1273 K. This value is representative of temperatures which have been given in Table 2. Values measured during tests 16 and 17 were much smaller than 1273 K. Infrared measurements may have underrepresented actual values because the small areas of flames associated with these tests did not offer an effective target for the infrared gun.

Values of h/D_o, α_B and A/D_o^2 observed during the Acheson field trials were compared to predicted values. Predicted values for each of the tests are shown in Table 14. This table also presents observed values together with standard deviations for tests conducted during evening hours.

Results from three of the evening tests were invalid. Pictures from two of these tests (no.'s 7, 8) were taken during times when fuel flows to the flare stack were being adjusted and the flame was not stable. This instability was reflected in the large standard deviations of observed α_B values. Pictures during the other test (no. 12) were taken while the pilots were active. Fuel injection from pilot nozzles affected flame behaviour.

Figure 8 shows a plot of predicted and observed values of normalized plume rise for the valid evening tests. The agreement is substantial and consistent with results attained with wind tunnel data.

Comparisons between observed and predicted α_B values are shown in Figure 9. Theory tended on average to overestimate α_B by

Table 13. Comparison between Predicted and Observed Values of α_B (Degrees) for Indicated Gases.

	n	Average Observed α_B	σ	Average Predicted α_B	SE	r
Methane	8	57	9.2	40	17.9	0.00
Butane	8	70	5.7	80	10.1	0.00
Ethylene	33	71	9.6	67	5.7	0.80
Propane	52	61	13.0	67	6.1	0.88
All Gases Except Methane	93	66	12.3	68	6.4	0.85

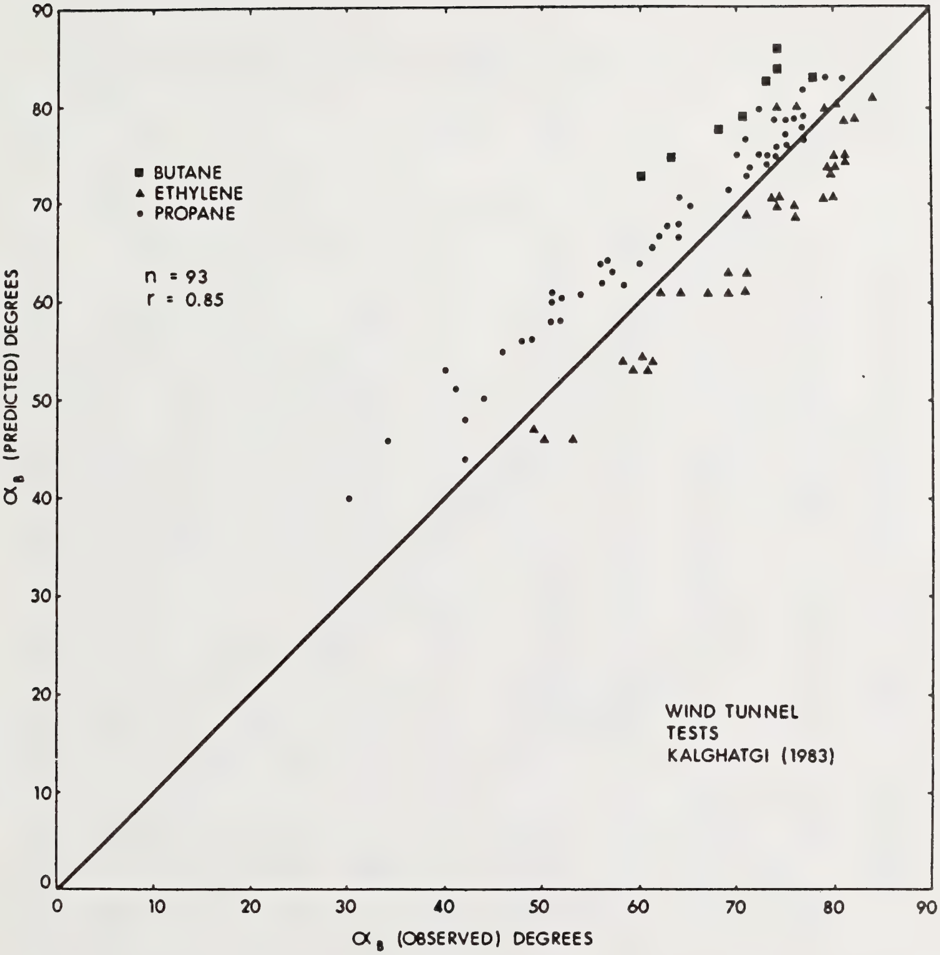

Figure 7. Comparison Between Predicted and Observed Values of α_B (Wind Tunnel Data). (Kalghatgi 1983).

Table 14. Observed and Predicted Values of h_f/D_o, α_B and A/D_o^2 Together with Associated Values of R, β_o and n (Present Theory).

				h_f/D_o		α_B (degrees)		A/D_o^2	
Test	R	β_o	n	Obs.	Pred.	Obs.	Pred.	Obs.	Pred.
1	0.85	1.42	NA[a]	NA	2	NA	83	NA	89
2	0.75	1.30	NA	NA	2	NA	79	NA	54
3	0.50	1.00	NA	NA	3	NA	76	NA	89
4	0.17	0.60	11	10 ± 3	11	54 ± 6	59	380 ± 30	224
5	0.20	0.64	10	10 ± 2	9	51 ± 8	61	280 ± 30	170
6	0.23	0.68	8	8 ± 1	7	53 ± 5	60	170 ± 10	116
7[b]	0.20	0.60	11	1 ± 2	9	59 ± 61	58	520 ± 50	142
8[b]	0.17	0.64	10	4 ± 2	9	55 ± 18	53	480 ± 50	134
9	0.21	0.65	NA	NA	9	NA	65	NA	231
10	0.21	0.65	NA	NA	8	NA	57	NA	116
11	0.19	0.63	NA	NA	7	NA	46	NA	62
12[b]	0.56	1.07	10	6 ± 1	2	38 ± 3	65	70 ± 10	18
13	0.33	0.80	10	9 ± 3	6	64 ± 10	74	410 ± 50	187
14	0.48	0.98	10	4 ± 0	4	73 ± 2	76	190 ± 10	100
15	0.52	1.02	10	4 ± 2	3	72 ± 10	74	160 ± 30	62
16	0.69	1.23	10	2 ± 1	2	68 ± 12	69	80 ± 20	18
17	0.53	1.03	10	2 ± 2	3	70 ± 11	71	80 ± 30	45

[a] NA = Not applicable

[b] Invalid tests

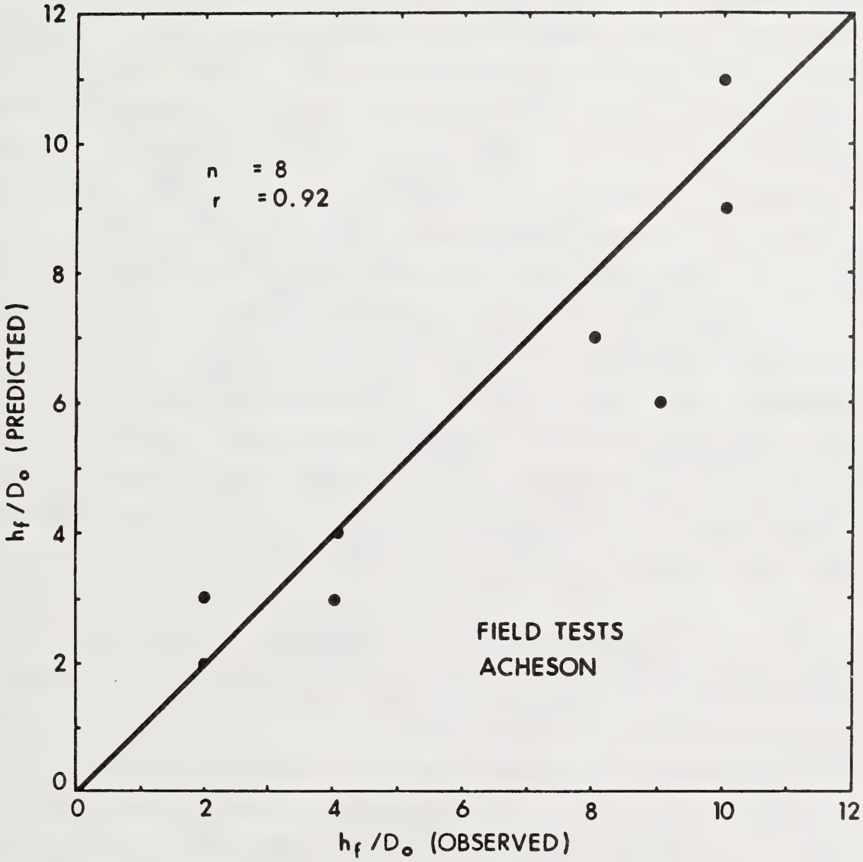

Figure 8. Comparison Between Predicted and Observed Values of h_f/D_o (Field Tests).

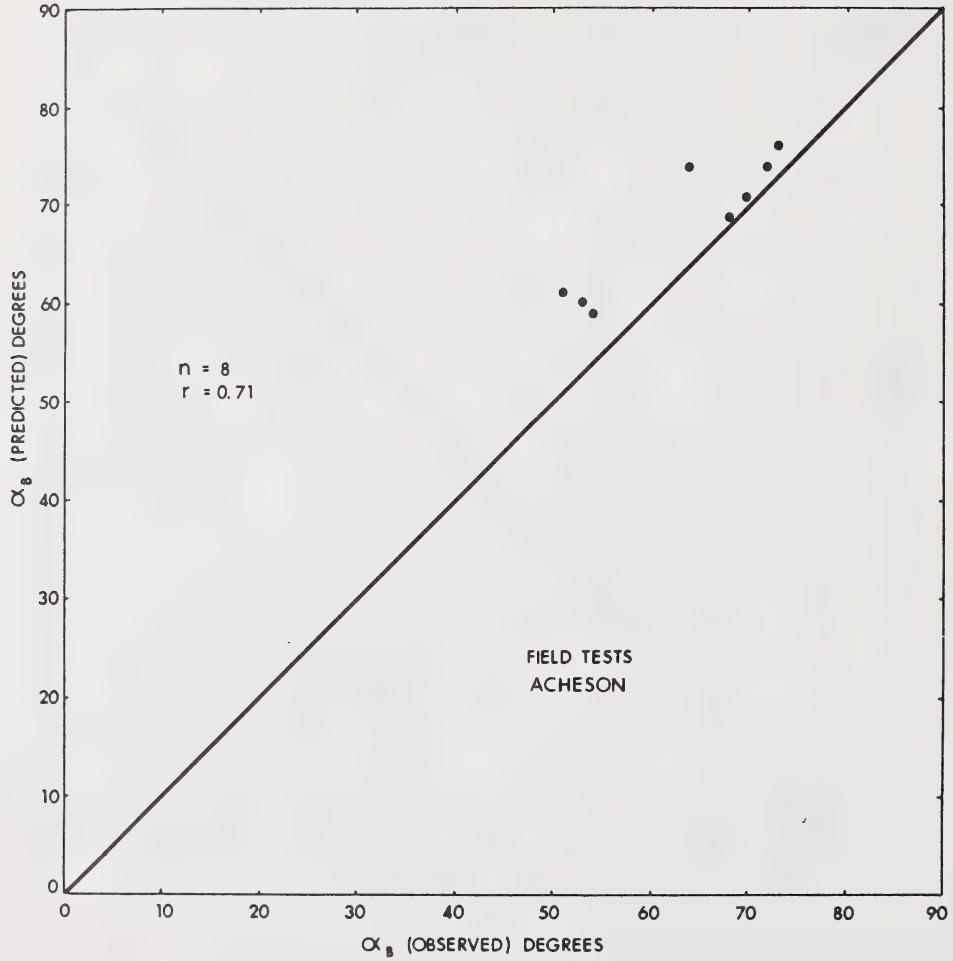

Figure 9. Comparison Between Predicted and Observed Values of α_B.

about five degrees. The correlation coefficient is relatively small. Part of the explanation lies in the small range of values contained in the population sample.

Table 14 shows that observed plume areas were substantially larger than predicted. The explanation for this probably lies in the downwash phenomenon, whereby exiting gases are entrained in eddies generated on the leeward side of the stack (Hanna et al. 1982). This phenomenon is illustrated in the comparison between predicted and observed cross-sectional areas presented in Figure 10. The appreciable area shown below the theoretical plume could be mostly due to downwash influences.

If the plume area was enlarged by downwash, it could be directly proportional to the theoretical area. The proportionality constant, ratio of average observed to average predicted areas, is 1.9. Figure 11 compares observed areas and predicted areas as revised by multiplication by 1.9. There is very good agreement between predicted and observed areas. The implication of this result is that visual observation of downwash probably give a pessimistic picture of its quantitative effect. The same conclusion was reached by Moore (1974) from studies of plume rises from a power plant stack.

Kalghatgi's equations (2) and (3) were also evaluated for each of the Acheson evening tests. Equation (2) was applied with the assumption that the molecular weight of the flare gas was 36. Observations indicated an actual average molecular weight of the flare gases tested during the day to be 36 with a standard deviation of 3. Results of the evaluation presented in Table 15 showed that Kalghatgi's theory tended to overestimate both h_f/D_o and α_B. There was no correlation between predicted and observed values.

3.5 FLAME EFFICIENCIES THROUGH MODEL USE

It has been postulated that flare efficiencies will be functions of the ratio of actual flame volume (V_o') to the volume (V_o) needed to ensure complete combustion. According to equation

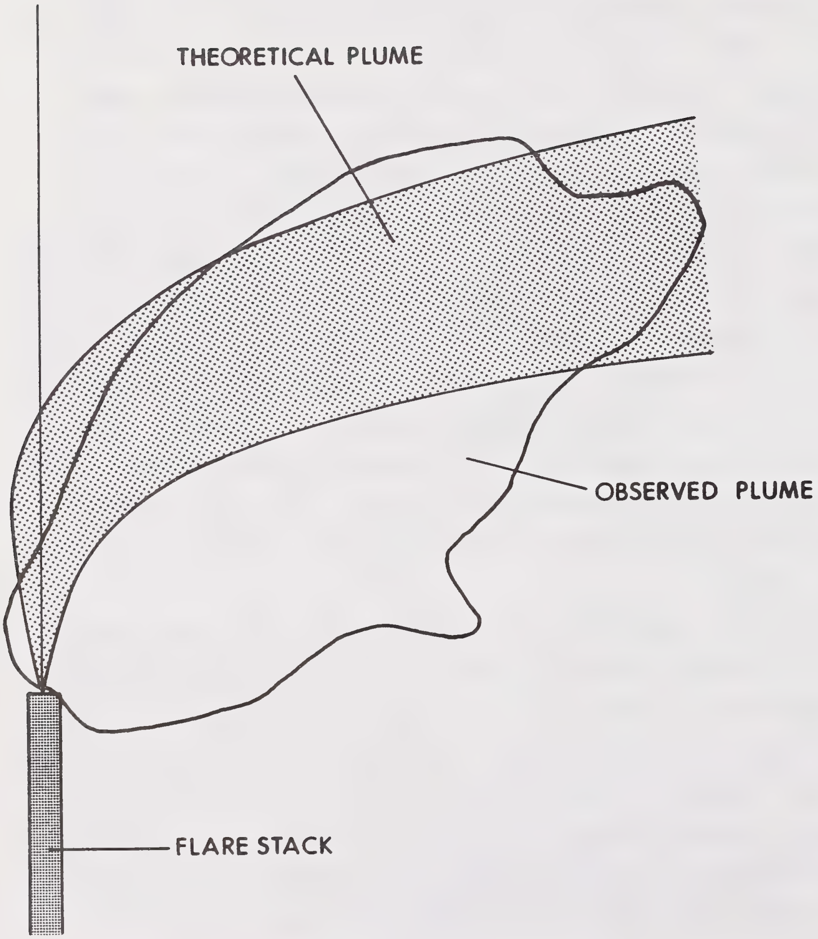

Figure 10. Illustrative Comparison Between Theoretical and Observed Flames.

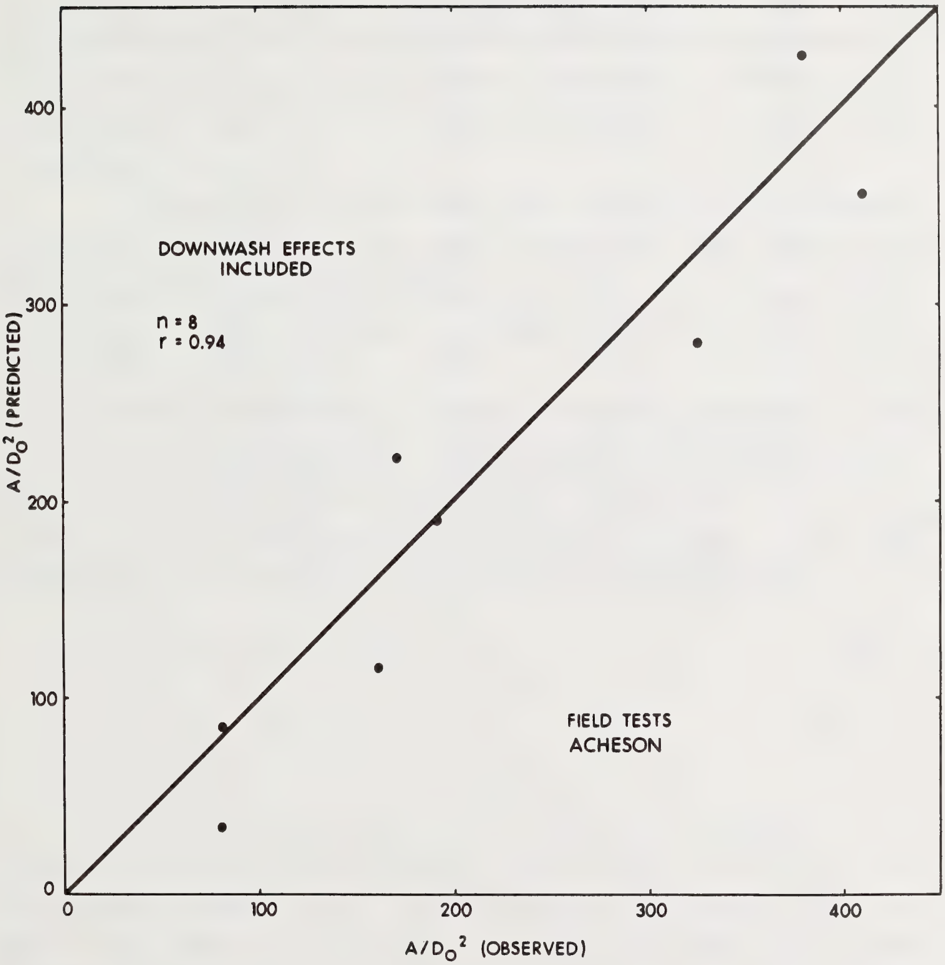

Figure 11. Comparison Between Predicted and Observed Values (Adjusted for Downwash Effects) of A/D_O^2.

Table 15. Observed and Predicted Values of h_f/D_o and α_B, Using Kalghatgi's Theory (1983)

Test	R	h_f/D_o Observed	h_f/D_o Predicted	α_B degrees Observed	α_B degrees Predicted
4	0.17	10 ± 3	9	54 ± 6	79
5	0.20	10 ± 2	9	51 ± 8	79
6	0.23	8 ± 1	10	53 ± 5	79
13	0.33	9 ± 3	12	64 ± 10	78
14	0.48	4 ± 0	15	73 ± 2	74
15	0.52	4 ± 2	16	72 ± 10	73
16	0.69	2 ± 1	19	68 ± 12	68
17	0.53	2 ± 2	16	70 ± 11	72
Mean		6.1 ± 3	13 ± 4	63 ± 9	75 ± 4

(6), the latter volume is a function of flame area (A) and downwind extent of the flame (x_f). As V_o', A, and x_f are all functions of R and β_o, it follows that flare efficiency must also be a function of these parameters which observation shows can vary by a factor of 3 over short time periods. If follows that flare efficiencies will also be subject to rapid fluctuation with time. For this reason, a nearly instantaneous measurement of efficiency, such as those attained in this study may not be representative of longer time averages.

Efficiencies as observed over a time period of several seconds were correlated with heat content (H), heat flux (πD_o^2 HV), flame area (A), flame volume (V_o), and V_o'/V_o ratios. Areas and volumes of the flames were estimated using typical values of β_o as given in equation (7).

Table 16 presents a comparison between values of E, as observed 2 m downwind of the Acheson stack and selected parameters. Linear correlation coefficients between the four valid values of E and associated heat contents and heat fluxes were about 0.90. Corresponding linear regression equations are:

$$E = 8H - 28.7; \text{ and} \tag{16}$$

$$E = 27.9\ (\pi\ D_o^2\ HV) - 4.2 \tag{17}$$

The high correlation coefficients are misleading as they were achieved by fitting a straight line to only four points. If, for example, Equation (16) is taken at face value then it follows that heat contents of 9 MJ·m^{-3} will be associated with flame combustion efficiencies of only about 45 percent. It would seem as though Alberta Environment's guideline, used for flare design is wholly inadequate. Such a conclusion is not born out from casual experience which shows that many operating sour gas flares in Alberta, designed according to the 9 MJ·m^{-3} criteria, are often odourless.

Table 16. Comparison Between Efficiencies E as Observed at Downwind Distances of 2 m and Selected Parameters.

Test	E Percent	H $MJ \cdot m^{-3}$	$\pi D_o{}^2 HV$ $MJ \cdot s^{-1}$	A m^2	$V_o{}'$ m^3	$V_o{}'/V_o$ Percent
1	96	16.8	3.8	1.8	0.05	36
2	g[a]	11.5	2.1	1.1	0.03	43
3	100[b]	13.3	2.7	1.8	0.06	50
9	100	16.2	3.9	4.6	0.26	100
10	89	11.9	2.5	2.3	0.11	62
11	22	7.9	1.4	1.2	0.06	75

[a] g = Flame out

[b] Suspect

Linear correlations between E and values of A and V_0' were relatively low at about 0.6 and 0.5, respectively.

The correlation between E and values of V_0'/V_0 was very low. This may have been because the instantaneous values of β_0 and R were not the same as those assumed in the calculations. The theory would have been better evaluated using the average of many efficiencies observed under the same stack exit conditions and wind speeds. There appears, however, to have been general agreement between values of E and V_0'/V_0. Thus, during tests 1-3 when volume ratios were relatively low flames tended to go out or were difficult to measure. During tests 9-11, when the ratios were greater, flames tended to be more evident and persistent. Complete combustion efficiency was reliably observed on only one occasion (Test 9). This is in agreement with the theory presented in this report which shows the combination of stack and meteorological parameters needed for complete combustion should be relatively rare.

4. CONCLUSION

The primary purpose of this study was to evaluate flares as an efficient means of combustion. Secondary purposes related to the measurements of mercaptans and heavy metals in flare gas streams and flaring practices as assessed through interviews with plant operators.

4.1 FLARE EFFICIENCIES

Flame combustion efficiencies were assessed using plume combustion data measured at Acheson. Estimated efficiencies at distances downwind of the flame in four valid tests were: 95.8, 100.0, 89.1 and 22.3 percent.

A model was proposed for purposes of explaining flare combustion efficiencies. The model is based upon the principle of energy conservation. Using this principle and the assumption of constant flame temperature, it was shown that complete combustion results in raising a given volume of gas from ambient to flame temperatures. Combustion will be less than 100 percent if flame volumes differ from this amount.

Flame dimensions have been demonstrated to be functions of stack exit and meteorological parameters which can vary rapidly in time. Associated combustion efficiencies because they are directly related to flame volumes will also be functions of these parameters. They must also be variable over short time periods.

4.2 MERCAPTANS AND HEAVY METALS

Concentrations of mercaptans in the acid gas and flare plume were always less than 0.03 and 0.003 percent, respectively. There were no mercaptans detected in the fuel gas. Concentrations of total heavy metals in the feed gas stream were small being less than about 250 $\mu g \cdot m^{-3}$.

4.3 INTERVIEWS OF SOUR GAS PLANT OPERATORS

Results of a brief survey of sour gas plant operators showed that many were unaware of the requirement that flare gas heat contents always be greater than 9 $MJ \cdot m^{-3}$. Success of combustion processes are only measured by the presence or absence of a flame. The tendency of the flame to be barely visible during the day often makes this simple test difficult to apply without the use of thermocouples.

Inexpensive measuring devices, such as Tutweiler absorption, GeoTech, or Draeger tubes are used on a weekly basis to estimate H_2S contents at smaller plants. More precise estimations using gas chromatography are routinely applied up to three times a week at larger plants. Estimates of the amount of H_2S flared is usually based upon a knowledge of the volume flow of acid gas as determined by an orifice meter. However, at some plants, operators estimate the volume flow of H_2S from estimates of flows from individual wells.

5. RECOMMENDATIONS

The preliminary investigations described in this report should be extended. It is specifically recommended that:

(1) The theory developed in this preliminary report be more fully evaluated. Additional testing could be accomplished by using field data available from studies conducted in the United States, Germany and elsewhere.

(2) The theory developed in this report be extended to predict flame parameters for gases of small molecular weights, such as methane.

(3) A low flare stack be established on the grounds of an existing sour gas plant. This would facilitate verification of sampling procedures and model predictions.

(4) An intensive study be made on the use of various desiccants in the presence of trace species in gas streams.

(5) Detailed surveys be made of all sour gas plant operators to determine their awareness of potential combustion problems associated with flaring.

(6) Reviews be made concerning the frequency of emergency flaring.

(7) Appraisals be made of the amount of sour gas vented up emergency flare stacks.

(8) Assessments be made of alternate means of combustion of H_2S.

7. REFERENCES CITED

Alberta Environment. 1982. Industrial Sulphur Emissions for Alberta 1977-1981. Air Quality Control Branch, Pollution Control Division, Alberta Environment, Edmonton.

Becker, H.A. and D. Liang. 1978. Visible length of vertical free turbulent diffusion flames. Combustion Flame 32: 115-137.

Beychok, M.R. 1979. Fundamentals of stack gas dispersion, Milton R. Beychuk, 63 Oaktree Lane, Irvine, Ca 92715.

Briggs, G.A. 1975. Plume rise predictions. Lectures on Air Pollution and Environmental Impact Analyses, American Meteorological Society, 34 Beacon Street, Boston, Massachusetts 02108 U.S.A.

Brzustowski, T.A. 1972. A model for predicting the shapes and lengths of turbulent diffusion flames over elevated industrial flares. Presented at the 22nd Canadian Chemical Engineering Conference, Toronto, Sept. 17-22, 1972.

Brzustowski, T.A. 1973. A new criteria for the length of a gaseous turbulent diffusion flame. Combustion Science and Technology 6: 313-319.

Brzustowski, T.A. 1975. The turbulent diffusion flame in a cross wind. Proceedings of the Fifth Canadian Congress of Applied Mechanics, Fredericton, May 26-30, 1975.

Brzustowski, T.A. 1976. Flaring in the energy industry. Progress in Energy Combustion Science. pp. 129-141.

Brzustowski, T.A. 1977. Flare testing and safety. Loss Prevention 11: 23-30.

Brzustowski, T.A., S.R. Gollahalli, M.P. Gupta, M. Kaptein, H.F. Sullivan. 1975. Radiant heating from flares. ASME paper 75-HT-4.

Dubnowski, J.J. and B.C. Davis. 1983. Flaring combustion efficiency: a review of the state of current knowledge. Paper presented at the 16th Annual Meeting of the Air Pollution Control Association, Atlanta, Georgia.

Engineering Science. 1983. A report on a flare efficiency study. Prepared for Chemical Manufacturers Association, Washington, D.C.: pp 133.

Escudier, M.P. 1972. Aerodynamics of a burning turbulent gas jet in a crossflow. Combustion Science and Technology 4: 293-301.

Gollahalli, S.R. 1977. Effects of diluents on the flame structure and radiation of propane jet flames in a concentric stream. Combustion Science and Technology 15: 147-160.

Gollahalli, S.R., T.A. Brzustowski, H.F. Sullivan. 1975. Characteristics of a turbulent propane diffusion flame in a cross wind. Transactions CSME 3: 205-214.

Hajek, J.D. and E.E. Ludwig. 1960. How to design safe flare stacks. Petro/Chem. Engineer Pt. XXXII C31-38 and Pt. 2 XXXII C44-51.

Halitsky, J. 1961. Single-camera measurement of smoke plumes. Atmospheric Environment 4: 185-198.

Herget, W.F. 1978. Remote measurement of off-gas flare combustion efficiency. EPA Report, September 26, 1978. (Original not seen, information taken from Dubnowski and Davis 1983.)

Howes, J. et al. 1981. Draft final report on development of flare emissions measurement methodology. EPA Contract No. 68-02-2682, Task Directive 118, August 14, 1984. (Original not seen, information taken from Dubnowski and Davis 1983.)

Joseph, D., J. Lee, C. McKinnon, R. Payne and J. Pohl. 1983. Evaluation of the efficiency of industrial flares used to destroy waste gases. Final report, EPA contract No. 68-02-3661, 1983.

Kalghatgi, G.T. 1983. The visible shape and size of a turbulent hydrocarbon jet diffusion flame in a cross wind. Combustion and Flame 52: 91-106.

Kent, G.P. 1964. Find radiation effect of flares. Hydrocarbon Processing 47: 119-130.

Kerr, R.K., H.G. Paskall and L.C. Biswanger. 1975. "Sulphur Plant Waste Gases: Incineration Kinetics and Fuel Consumption". Alberta Environment, Edmonton.

Leahey, D.M. and M.J.E. Davies. 1984. Observations of plume rise from sour gas flares. Atmospheric Environment 18: 917-922.

Lee, K. and G.M. Whipple. 1981. Waste gaseous hydrocarbon combustion in a flare. 74th Air Pollution Control Association Meeting, Phila., Pa., June 21-26, 1981.

Lewis, Bernard and Guenther Von Elbe. 1961. Combustion flames and explosions of gases. Academic Press Inc., New York and London.

Masliyah, J.A. and F.R. Steward. 1969. Radiative heat transfer from a turbulent diffusion buoyant flame with mixing controlled combustion. Combustion and Flame 13: 613-625.

McDaniel, M.D. 1983. A report on a flare efficiency study. Prepared for the Chemical Manufacturers Assocation, March, 1983.

Moore, D.J. 1974. The prediction of the mean hourly average maximum ground level concentration of sulphur dioxide at Tilbury. Atmospheric Environment 8: 543-554.

Morton, B.R. 1965. Modeling fire plumes. Tenth Symposium (International) on Combustion pp. 973-982.

Palmer, P.A. 1972. A tracer technique for determining efficiency of an elevated flare. Unpublished report. (Original not seen, information taken from Dubnowski and Davis 1983.)

Oenbring, P.R. and T.R. Sifferman. 1980. Flare design - are current methods too conservative? Hydrocarbon Processing. 124-129.

Paskall, H. 1974. "Determination of Trace Metals in Sulphur Plant Stack Gases". Letter report to Alberta Environment (J. Defir).

Ricou, F.P. and D.B. Spalding. 1961. Measurements of Entrainment by Axisymettrical Turbulent Jets. Journal Fluid Mechanics 9 pp. 21-32.

Siegel, K.D. 1980. Degree of conversion of flare gas in refinery high flares. Thesis, PhD in Engr. Science, Chemical Engr. Dept., Univ. of Karlesruhe, Germany, February, 1980. (Original not seen, information taken from Dubnowski and Davis 1983).

Steward, F.R. 1970. Prediction of the height of turbulent diffusion buoyant flames. Combustion Science and Technology 2: 203-212.

Straitz, J.F. 1978. Flaring for gaseous control in the petroleum industry. 1978 Annual APCA Meeting, June 29, 1978.

Tan, S.H. 1967. Flare system design simplified. Hydrocarbon Processing 46: 172-176.

Thimm, H.F. 1984. Senior Technical Advisor, Alberta Energy Resources Conservation Board, Calgary. Personal Communication.

Townsend, A.A. 1966. The mechanism of entrainment in free turbulent flows. Journal Fluid Mechanics 26: 689-697.

Zabetakis, M.G. and D.S. Burgess. 1961. Research in hazards associated with the production and handling of liquid hydrogen. RI 5707, Dept. of the Interior, U.S. Bureau of Mines.

7. APPENDICES

7.1 Appendix A

Information relating to raw data and calibration.

Table A1: Metal Analyses (unedited) as Supplied by Metro-Tech Systems Ltd.

Table A2: Summary of Chemical Absorption Data on Flare Feed Streams

Figure A1: Sample of Actual Chromatograph Output For Acid Gas Analysis

Figure A2: Sample of Actual Chromatograph Output For Plume Analysis

Gas chromatograph calibration check

TABLE A1

276-9431
276-9432

MAR. 13, 1984 WESTERN RESEARCH Re: I.G.G. - ACHESON (5031)

OUR SAMPLE NO	BLANK	FUEL GAS #1	FUEL GAS #2	FUEL GAS #3	ACID GAS #1	ACID GAS #2
UR SAMPLE NO	1234	1203	1204	1205	1206	1207
	P.P.M.	P.P.M.	P.P.M.	P.P.M.	P.P.M.	P.P.M.
ILVER	<4PPB	<4PPB	<4PPB	<4PPB	<4PPB	<4PPB
LUMINUM	<15PPB	<15PPB	0.014	<15PPB	<15PPB	<15PPB
RSENIC	<25PPB	<25PPB	<25PPB	<25PPB	<25PPB	<25PPB
ORON	<5PPB	<5PPB	<5PPB	<5PPB	<5PPB	<5PPB
ARIUM	<0.2PPB	0.0006	<0.2PPB	<0.2PPB	<0.2PPB	<0.2PPB
ALCIUM	<0.2PPB	<0.2PPB	<0.2PPB	<0.2PPB	<0.2PPB	<0.2PPB
ADMIUM	<1PPB	<1PPB	<1PPB	<1PPB	<1PPB	0.002
HROMIUM	<4PPB	<4PPB	<4PPB	<4PPB	<4PPB	<4PPB
OPPER	<2PPB	0.065	<2PPB	<2PPB	<2PPB	<2PPB
RON	0.105	0.130	<2PPB	0.022	<2PPB	0.020
ERCURY	—	1.0 PPB	0.7 PPB	1.0 PPB	0.5 PPB	3.4 PPB
OTASSIUM	<125PPB	<125PPB	<125PPB	<125PPB	<125PPB	<125PPB
AGNESIUM	<0.2PPB	<0.2PPB	<0.2PPB	<0.2PPB	<0.2PPB	<0.2PPB
ANGANESE	<0.5PPB	<0.5PPB	<0.5PPB	<0.5PPB	<0.5PPB	<0.5PPB
OLYBDENUM	<5PPB	<5PPB	<5PPB	<5PPB	<5PPB	<5PPB
ODIUM	<10PPB	0.613 *	5.49 *	<10PPB	<10PPB	1645. *
CKEL	<6PPB	<6PPB	0.021	<6PPB	<6PPB	<6PPB
IOSPHOROUS	0.031	<30PPB	<30PPB	<30PPB	<30PPB	0.440
AD	<20PPB	<20PPB	<20PPB	0.020	<20PPB	0.008
LENIUM	<20PPB	<20PPB	<20PPB	<20PPB	<20PPB	<20PPB
LICON	<10PPB	<10PPB	<10PPB	<10PPB	<10PPB	<10PPB
N	<6PPB	<6PPB	<6PPB	<6PPB	<6PPB	<6PPB
ANIUM	—	—	—	—	—	—
NADIUM	<2PPB	<2PPB	<2PPB	<2PPB	<2PPB	<2PPB
NC	<2PPB	0.021	0.007	0.095	0.009	<2PPB
RYLLIUM	<0.3PPB	<0.3PPB	<0.3PPB	<0.3PPB	<0.3PPB	<0.3PPB

* CONTAMINATON FROM NaOH Scrubber.

TABLE A1 (continued)

276-9431
276-9432

MAR. 13, 1984 WESTERN RESEARCH - Re: I.C.G. - ACHESON (5031

YOUR SAMPLE NO	ACID GAS #3
OUR SAMPLE NO	1208
	P.P.M.
SILVER	<4 PPB
ALUMINUM	<15 PPB
ARSENIC	<25 PPB
BORON	<5 PPB
BARIUM	<0.2 PPB
CALCIUM	<0.2 PPB
CADMIUM	<1 PPB
CHROMIUM	<4 PPB
COPPER	<2 PPB
IRON	<2 PPB
MERCURY	<0.5 PPB
POTASSIUM	<125 PPB
MAGNESIUM	<0.2 PPB
MANGANESE	<0.5 PPB
MOLYBDENUM	<5 PPB
SODIUM	2850*
NICKEL	<6 PPB
PHOSPHOROUS	0.030
LEAD	<20 PPB
SELENIUM	<20 PPB
SILICON	<10 PPB
TIN	<6 PPB
URANIUM	—
VANADIUM	<2 PPB
ZINC	0.017
BERYLLIUM	<0.3 PPB

Numbers without units indicate ppm (mg/L of Soluti)

(other numbers indicate minimum detectable Limits)

Analysis by
Metro-Tech Systems
Ltd., Calgary

Table A2. Summary of Metal Absorption Data on Flare Feed Streams.

Acheson Gas Plant 1984-03-06

Stream	Start/ Stop	Average Meter Temperature (°F)	Average Dry Impinger Pressure (in Hg)	Dry Gas Metered (ft^3)	Final Solution Volume (mL)[b]	Wash Solution Added (mL)
Acid Gas						
(1)	10:03 11:03	47.1	-7.09	0.445 0.463[a]	211.0[c]	50.0
(2)	11:34 12:34	47.7	-5.49	0.339 0.353[a]	220.5	50.0
(3)	13:32 14:32	48.6	-6.10	0.224 0.223[a]	219.0	50.0
Fuel Gas						
(1)	15:14 16:14	45.0	-2.31	12.684 13.191[a]	200.0	52.0
(2)	16:31 17:31	40.2	-1.93	10.546 10.968[a]	200.0	50.0
(3)	17:40 18:40	37.4	-1.94	6.899 7.175[a]	200.0	50.0

[a] Corrected according to meter recalibration factor of 1.040

[b] The initial volume in each case was 200.0 mL, barometric pressure, 27.48 in Hg.

[c] Third impinger contents discarded because of contamination with NaOH.

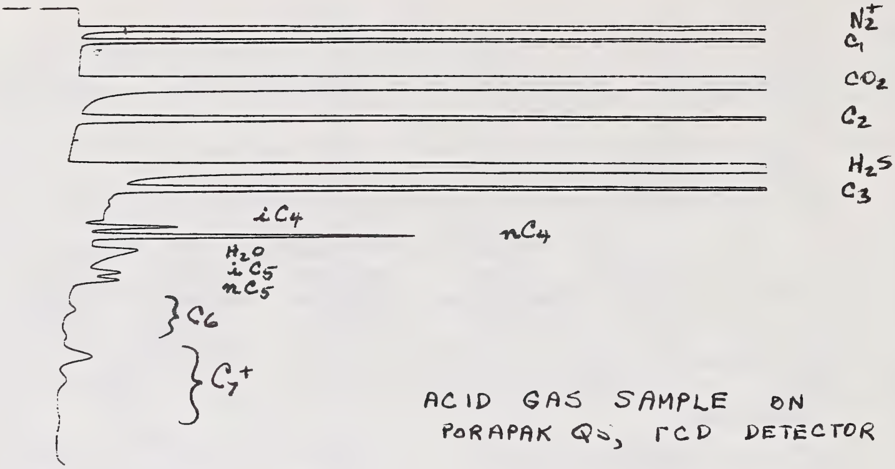

ACID GAS SAMPLE ON PORAPAK QS, TCD DETECTOR

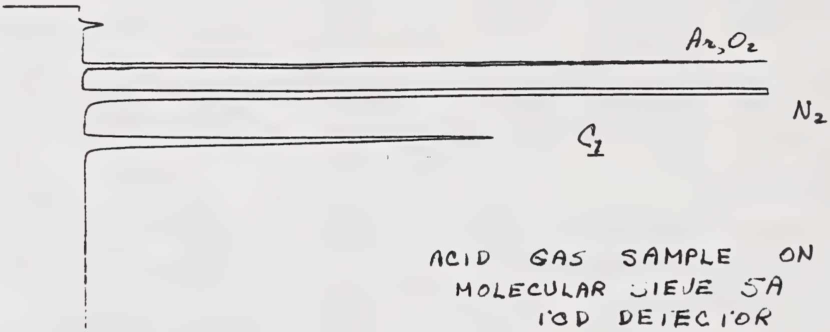

ACID GAS SAMPLE ON MOLECULAR SIEVE 5A TCD DETECTOR

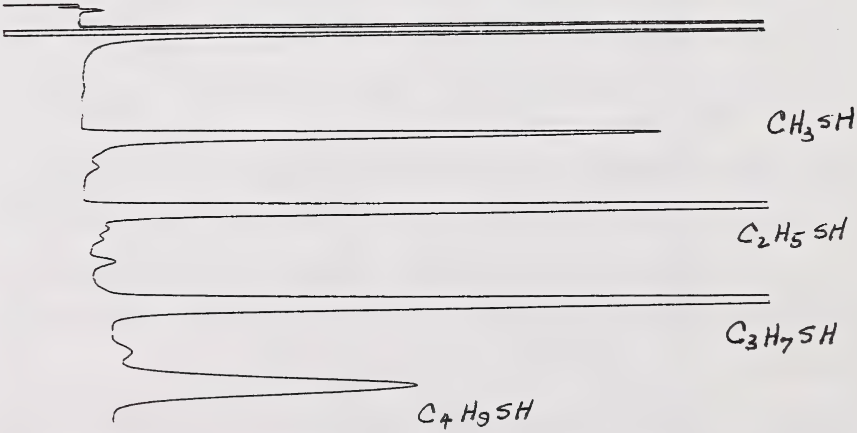

ACID GAS SAMPLE ON PORAPAK QS, PID DETECTOR

Figure A1

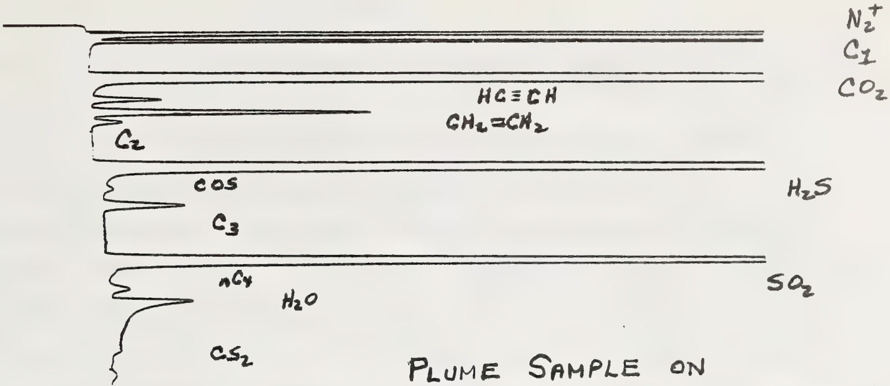

PLUME SAMPLE ON
PORAPAK QS, TCD DETECTOR

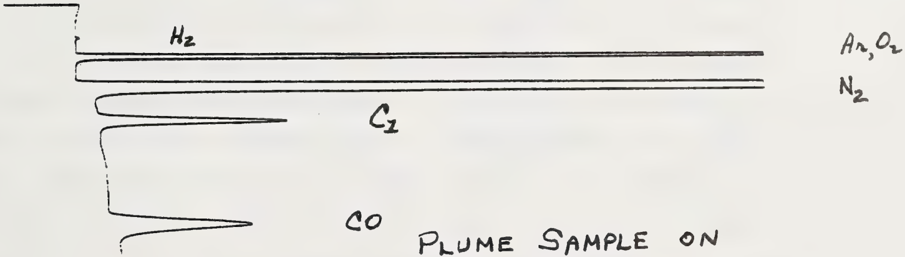

PLUME SAMPLE ON
MOLECULAR SIEVE 5A
TCD DETECTOR

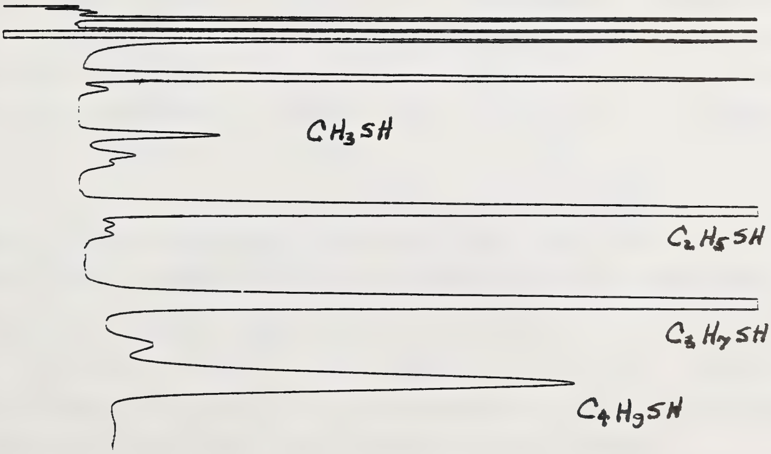

PLUME SAMPLE ON
PORAPAK QS, PID DETECTOR.

Figure A2

1. GAS CHROMATOGRAPH CALIBRATION CHECK

1.1 THERMAL CONDUCTIVITY DETECTOR

Calibration curves for the thermal conductivity detector (T.C.D) were prepared for all components of interest using a mole ratio method. Because response of the thermal conductivity detector to CO_2 is linear over a wide dynamic range, and CO_2 is a major component of many samples, CO_2 was chosen as the calibration reference gas, and assigned a relative response factor of unity. To calibrate for a given component, X, a binary mixture of CO_2 and X was prepared by mass for primary calibrations and by partial pressure for calibration checks. X is obtained by doing multiple injections of different sample sizes, and constructing a calibration curve for the entire range, from the limit of detectability to the saturation point of the detector. In practice, more than one mixture with various X/CO_2 molar ratios were used. Data were fitted by a least squares method to an equation of the form $M=aA^b$ exp [cA] where M is relative molar units of X; A is peak area given by M; and a, b, and c are the calibration factors for X.

A major component, CH_4, was chosen for a field calibration check on the thermal conductivity detector because it is impractical to perform a field calibration check on every component. Results of two multipoint runs are tabulated in Table A-3 and shown graphically in Figure A3. The check data were all within ±1.5 percent of the current calibration curve for CH_4.

1.2 PHOTOIONIZATION DETECTOR

For the photoionization detector field calibration check, the available mixture (Scott Specialty Gases, California) contained 99.4 ppm CH_3SH, 100.5 ppm $(CH_3)_2S$, and 99.9 ppm CH_3SSCH_3, with N_2 as balance gas. Because sulphides were not detected in any of the samples, only $(CH_3)_2S$ data were analyzed.

Repetitive runs before and after the field samples were tabulated in Table A-4.

Table A-3. Thermal Conductivity Detector Field Calibration Check ($GC\#8$, CH_4).

CO_2 Peak Area	CH_4 Peak Area	CH_4 Relative Molar Units: From Mix Data[a]	CH_4 Relative Molar Units: Calculated From Calibration Equation	CH_4 Relative Molar Units: Deviation (Percent)[b]
March 6, 1984				
304,437	1,628,630	2,500,776	2,524,300	-0.9
229,905	1,248,890	1,888,538	1,897,800	-0.5
201,797	1,102,840	1,657,647	1,662,400	-0.3
169,623	934,457	1,393,356	1,394,900	-0.1
134,635	748,450	1,105,950	1,104,300	+0.2
101,177	567,421	831,111	826,820	+0.5
March 9, 1984				
318,921	1,708,510	2,619,754	2,658,700	-1.5
286,402	1,507,600	2,352,629	2,355,600	-0.1
249,709	1,343,200	2,051,217	2,051,400	-0.01
217,134	1,175,900	1,783,632	1,779,700	+0.2
177,178	968,557	1,455,416	1,448,700	+0.5
138,891	767,552	1,140,910	1,133,900	+0.6
101,946	569,885	837,428	830,560	+0.8
36,708	210,906	301,535	297,120	+1.5

---

[a] Mixture contained 81.98 percent CH_4, 9.98 percent CO_2 with balance as N_2 (prepared with gas blender by partial pressure).

[b] Calibration curve as reference.

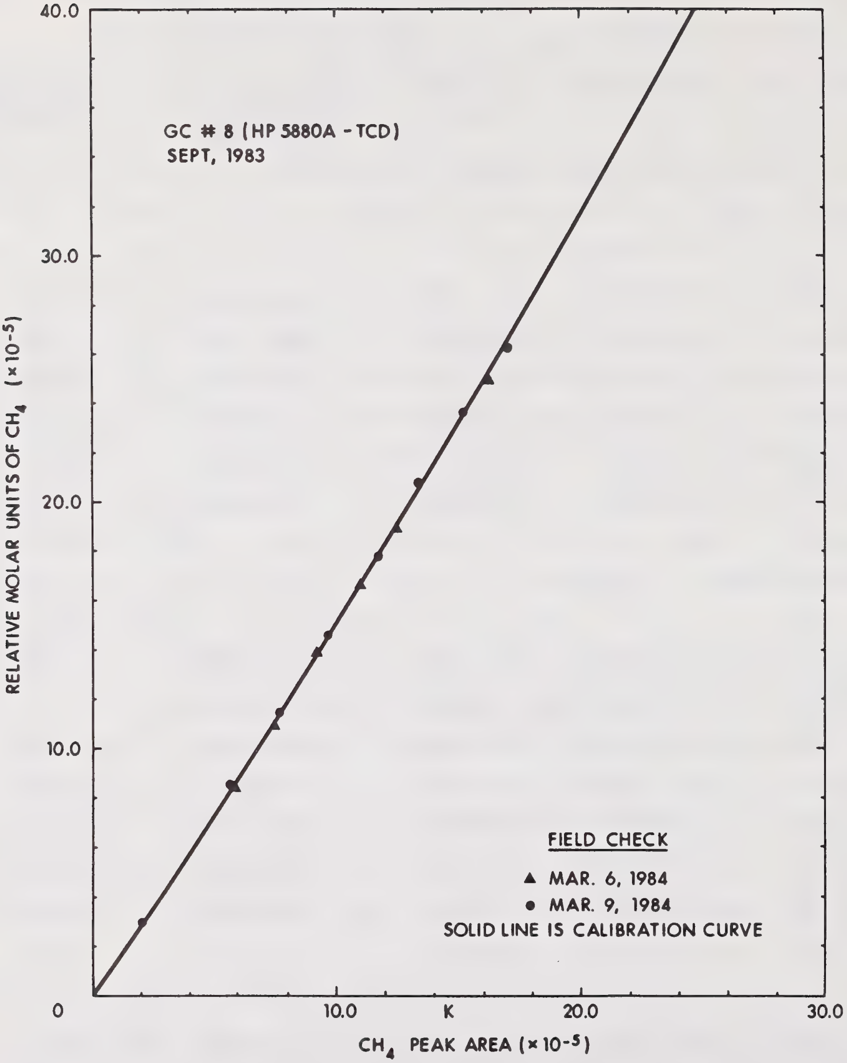

FIGURE A3. CH_4 CALIBRATION

Table A-4. CH_3SH Relative Response Factor Photoionization Detector.

Injection	CH_3SH Peak Area	CH_3SH Concentration (from average response factor) (ppm)	Relative Response Factor
March 6, 1984			
1	60255	102.8	
2	58299	99.5	
3	58625	100.0	
4	56338	96.1	
5	55809	95.2	
6	58516	99.8	
7	59976	102.3	1.706×10^{-3}
Mean	58260	99.4	
March 9, 1984			
1	58018	97.7	
2	59558	100.3	
3	61209	103.0	
4	57682	97.1	
5	61596	103.7	
6	57216	96.3	
7	58022	97.7	
Mean	59043	99.4	1.684×10^{-3}

For mercaptans, the photoionization detector is normally calibrated in the following manner. A calibration mixture containing CH_3SH is run prior to field samples and a response factor is calculated. Then, the concentrations of CH_3SH for the field samples are computed using the CH_3SH response factor. Concentrations of the remaining mercaptans are computed from previously measured responses relative to CH_3SH.

The relative response factors determined on the two days differed by less than 1.5 percent.

7.2 APPENDIX B

Questionnaire: Alberta Environment Flare Stack Emission Study.

TELEPHONE QUESTIONNAIRE LOG SHEET - JOB #3033
ALBERTA ENVIRONMENT FLARE STACK EMISSION STUDY

Interviewer: ____________________ Date: ____________________

Contact Name: ____________________ Position: ____________________

Company: ____________________

Location: ____________________

Phone No.: ____________________

---

1. Introductions

   a. Refer to Dave Onuczko's contact
   b. Repeat that we are interested about flaring activities

2. Flare System Description

   a. Number of flares (including flare pits) ____________________
   (continuous-low pressure, emergency-high pressure)

   b. Process streams to each ____________________

   ____

   ____

   c. Fuel gas for pilot Y / N, enrichment Y / N

   d. Flare Design Parameters

height	____________	____________
exit diameter	____________	____________
flare tip design (open pipe, shrouded)	____________	____________
manufacturer	____________	____________
liquid knockouts	____________	____________
pilot(s) (number, continuous)	____________	____________
steam injection	____________	____________
ingnitor system (manual, electric automatic)	____________	____________

Page 1 of 4

3. Flared Gas Volume Measurement

   a. Instruments used (orifice, positive displacement meter)

   b. Process streams measured (continuous and emergency)

   c. Fuel gas consumption record?

   d. Enrichment gas, how do they know how much to add?

      Are they aware of 9 MJ/m^3 guideline?

      How do they confirm it?

   e. Results reported to whom (ERCB, internal use)?

4. Flared Gas Composition

   a. Is composition of gases to flare measured?

      Which streams (continuous or emergency)?

   b. Method used (gas chromatograph, H_2S by Tutweiller, Draeger or GasTech)?

   c. Regularity of sampling (yearly, monthly)?

   d. Results reported to whom?

5. Monitoring of Flaring Activities

a. Method used (visual, mirrors, remote camera, thermocouple signal tied into alarm, sound of flare) ____________________

____

b. Describe typical flame (colour, size, smoke) for each flare

____

c. Are records kept of continuous flare performance (flame failures, excessive smoking, flows)? ____________________

d. Are records kept of emergency flaring incidents (cause, time, duration, flared volumes, smoking)? ____________________

e. Have more elaborate flare studies been done (IR thermometer, downwind H_2S surveillance)? ____________________

____

6. Problems Related to Flaring

a. Flame failures

Regularity ____________________

Cause (loss of fuel gas, line freeze-ups, liquid carryover, knockout overflow, erratic flare gas flow rates, high winds, rain) ____________________

____

____

b. Describe relighting procedure ____________________

____

c. Complaints: downwind odours (H_2S, SO_2, hydrocarbons), excessive smoking, flame visibility, grass or bush fires?

____

____

____

d. Any other problems? ______________________________

____

____

e. Routine inspection/servicing of flare ______________

____

f. Equipment changes to improve flare performance ________

____

____

7. Closing Statements

8. Note contacts attitude ______________________________

____

Page 4 of 4

7.3 APPENDIX C

Derivation of equations for plume rise, plume length and plume area.

The rise of a diffusion flame is influenced by momentum and buoyancy forces. It will be assumed for purposes of this study that buoyancy forces are negligible Escudier (1972). It will be further assumed that:

(1) Gas exits from the flare stack in a series of puffs which follow the same trajectory.

(2) Plumes resulting from integration of the puffs have a "top hat" profile. That is, a variable will have a certain constant value inside the plume, another value outside the plume and a discontinuity at the plume boundary.

(3) The diameter of the plume will be assumed to be proportional to plume rise i.e.:

$$D = 2\beta h; \qquad \text{(C1)}$$

where D = plume diameter,
h = plume rise, and
β = entrainment constant.

Conservation of mass and energy requirements can now be applied to the existing gas to show (Briggs 1975):

$$h = Kx^{1/3}; \qquad \text{(C2)}$$

$$K = \left[\frac{3}{4\beta^2}\right]^{1/3} \left[\frac{D_o}{R}\right]^{2/3} \left[\frac{\rho}{\rho_o}\right]^{1/3};$$

where x = downwind distance;
$R = U/V$;
U = wind speed;
V = stack exit speed;
β = entrainment constant;

D_o = stack diameter

ρ, ρ_o = density of flare gas and air respectively

Puffs of gaseous fuel will ignite and burn as they leave the flare stack. This ignition is assumed not to occur for puffs of fuel concentration less than the stoichiometric mixing ratio. For plumes with a top hat profile:

$$C_s = \frac{D_o^2\ V}{D_f^2\ U} \times 100; \tag{C3}$$

where C_s = stoichiometric mixing ratio (percent by vol.)

D_f = diameter of plume at the downwind distance where puff concentration equals C_s

Combining Eqs. (C1), (C2) and (C3) gives:

$$C_s = \frac{25\ D_o^2}{R\beta^2 K^2 x_f^{2/3}}; \tag{C4}$$

where: x_f = downwind extent of the flame

From Eqs. (C1), (C2) and (C4) it follows that:

$$h_f = \frac{5\ D_o}{\beta}\left[\frac{1}{RC_s}\right]^{\frac{1}{2}}; \tag{C5}$$

$$\frac{h_f}{x_f} = \frac{3}{4}\ \frac{1}{25}\left[\frac{\rho}{\rho_o}\right]\left[\frac{C_s}{R}\right]; \text{ or}$$

$$\frac{h_f}{x_f} = .03\left[\frac{\rho}{\rho_o}\right]\left[\frac{C_s}{R}\right]. \tag{C6}$$

Flared gas is emitted at relatively high speed into the atmosphere where flames will maintain high temperatures in the immediate vicinity of the flare stack exit. Gases leaving the flare stack will be subjected to forces created by dynamic pressures and heating. It will be assumed that the effective density of exiting gases will be equal to flame gas densities. Because of rapid mixing the molecular weight of the flame gas will be close to that of air. It follows that:

$$\frac{\rho}{\rho_0} \cong \frac{T_0}{T} \; ; \qquad \text{(C7)}$$

where: T_0 = temperature of air (K); and
T = temperature of flame (K).

Both experimental evidence (Ricou and Spalding 1961) and theory (Morton 1965; Townsend 1966) show that the rate of entrainment β for a jet whose density ρ is different from that of the surroundings (ρ_0) is given by:

$$\beta = \beta_0 \left[\frac{\rho}{\rho_0}\right]^{\frac{1}{2}} \; ; \qquad \text{(C8)}$$

where β_0 is the entrainment constant for a jet of density ρ_0.

Average values of the entrainment constant for jets of density ρ_0 vary with R according to the relation (Briggs 1975):

$$\beta_0 = 0.4 + 1.2.\ R \; ; \qquad \text{(C9)}$$

[Note: Briggs uses a value for R in his equation which is defined as the inverse of the parameter given in equation (9). Hence his equation is expressed as: $\beta_0 = 0.4 + 1.2\ R^{-1}$.]

Applying equations (C5), (C6), (C7), (C8) and (C9) it follows that:

$$\frac{h_f}{D_0} = \frac{5}{0.4 + 1.2R}\left[\frac{1}{kR}\right]^{\frac{1}{2}} \; ; \text{ and} \qquad \text{(C10)}$$

$$h_f/x_f = .0303\ k/R\ ; \qquad \text{(C11)}$$

where: $k = \frac{T_o\ C_s}{T}$.

The length of the flame L_f is given by the equation:

$$L_f = (x_f^2 + h_f^2)^{\frac{1}{2}};$$

or using equations (C8), (C10) and (C11):

$$L_f = (1089\ R^2/k^2 + 1)^{\frac{1}{2}}\ h_f.$$

Consider a surface element of the flame of width ds. Its cross-section is indicated by the shaded area in Figure C1. The area, dA, of this surface element is:

$$dA = \pi D(x)ds(x');$$

$$D(x) = 2\beta h(x);$$

$$ds(x') = dx' \left(1 + \left[\frac{dh'}{dx'}\right]^2\right)^{1/2} \quad ;$$

where D = plume diameter; and

h′(x′) = upper boundary of flame cross-section at x′.

The surface area of the flame is, therefore:

$$A = \pi \int_0^{x_f'} D[x(x')] \left(1 + \left[\frac{dh'}{dx'}\right]^2\right)^{1/2} dx' \ ; \text{ or}$$

$$A = \pi \int_0^{x_f} D(x) \left(1 + \left[\frac{dh'}{dx}\ \frac{dx}{dx'}\right]^2\right)^{1/2} \frac{dx'}{dx}\ dx\ . \qquad \text{(C12)}$$

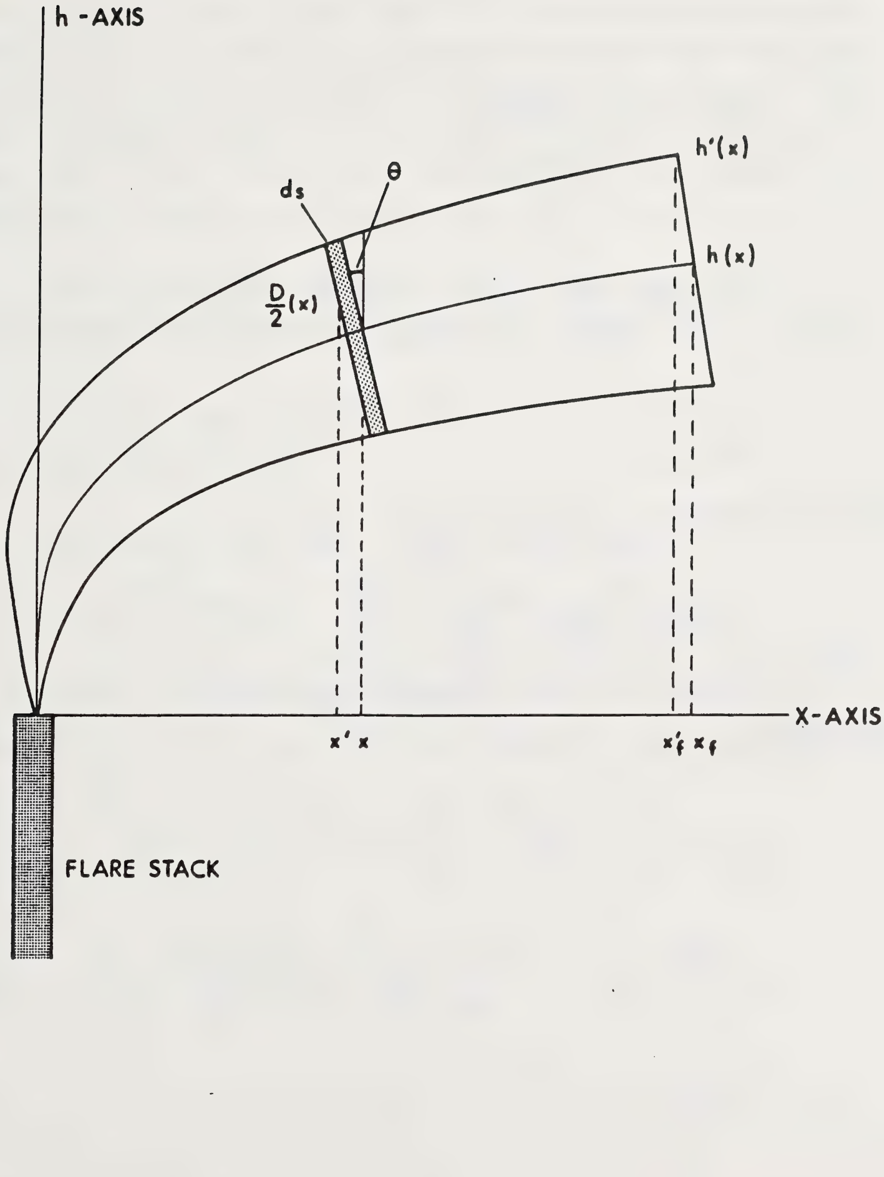

FIGURE C1 CROSS-SECTION OF THEORETICAL FLAME SHOWING PARAMETERS USED IN MATHEMATICAL DERIVATIONS

This integral can only be evaluated after determining the function $x'(x)$ from:

$$x - x' = \tfrac{1}{2}D(x)\sin\Theta(x);$$

where: $\tan\Theta = dh/dx$;

and using the fact that:

$$h'[x'(x)] = h(x) + \tfrac{1}{2}D(x)\cos\Theta(x).$$

The above leads to an integrand which is difficult to integrate. The integral is simplified with the assumptions:

$$h'[x'(x)] \cong h(x) + \tfrac{1}{2}D(x) = (1+\beta)\,h(x); \qquad (C13)$$

$$\text{where: } x \cong x'. \qquad (C14)$$

Then the approximate flame surface area is:

$$A \cong 2\pi\int_0^{x_f} \beta K x^{1/3}\left(1 + \frac{(1+\beta)^2}{9}K^2 x^{-4/3}\right)^{1/2} dx.$$

Evaluation of the integral and subsequent simplifications give:

$$\frac{A}{D_o^2} \cong \frac{3\pi}{2}\left[\frac{3}{4}\frac{T_o}{T}\right]^{1/3}\Bigg[\frac{\lambda}{\beta}\left\{\lambda^2 + \frac{(1+\beta)^2}{9}\left[\frac{3}{4}\frac{T_o}{T}\right]^{2/3}\frac{1}{R^2}\right\}^{1/2}$$

$$+\frac{(1+\beta)^2}{9}\left[\frac{3}{4}\frac{T_o}{T}\right]^{2/3}\frac{1}{\beta R^2}\log\Bigg\{\frac{3}{1+\beta}\left[\frac{4}{3}\frac{T}{T_o}\right]^{1/3}\Bigg[\lambda R + \Bigg(\lambda^2R^2$$

$$+\frac{(1+\beta)^2}{9}\left[\frac{3}{4}\frac{T_o}{T}\right]^{2/3}\Bigg)^{1/2}\Bigg]\Bigg\}\Bigg]; \text{ and}$$

$$\lambda = \left[\frac{500}{3}\frac{T}{T_o}\right]^{2/3}\frac{1}{C_s}.$$

Relative errors introduced by the approximations given in Equations (C13) and (C14) are less than 10 percent for $x/D_o > 1$ and $0.2 < R < 0.9$. This is the range of R values observed during the Acheson field experiments. Flame surface area near the stack ($x/D_o < 1$) does not contribute significantly to the total flame area. Therefore, Equation (C14) gives a satisfactory estimate of the total flame surface area for the present version of the theoretical flare model.

If $(dh'/dx')^2 << 1$ then Equation (C12) is simplified and consequential integration and manipulations show:

$$\frac{A}{D_o^{\,2}} \cong \frac{3927}{\beta_o C_s^{\,2}} \left[\frac{T}{T_o}\right]^{3/2} .$$

The volume of the flame is given by the equation:

$$V = \pi/4 \int_0^{x_f'} D^2 \left[x\ (x')\right] \left(1 + \left[\frac{dh'}{dx'}\right]^2 \right)^{1/2} dx'. \quad \text{(C15)}$$

Again, if $\frac{dh'}{dx'}{}^{2} << 1$, then (C15) with the use of equations (C1) and (C3), becomes:

$$\frac{V}{D_o^{\,3}} \cong \frac{7854}{\beta_o R^{1\ \ 2}} \left[\frac{T}{T_o}\right]^{3/2} \left[\frac{1}{C_s}\right]^{5/2} .$$

N.L.C. - B.N.C.
3 3286 06127824 4